Journal of Biomedical Optics

SPIEDigitalLibrary.org/jbo

Mitochondrial function and tissue vitality: bench-to-bedside real-time optical monitoring system

Avraham Mayevsky
Raphael Walden
Eliyahu Pewzner
Assaf Deutsch
Eitan Heldenberg
Jacob Lavee
Salis Tager
Erez Kachel
Ehud Raanani
Sergey Preisman
Violete Glauber
Eran Segal

SPIE

Mitochondrial function and tissue vitality: bench-to-bedside real-time optical monitoring system

Avraham Mayevsky,[a,b] Raphael Walden,[c] Eliyahu Pewzner,[b] Assaf Deutsch,[b] Eitan Heldenberg,[c] Jacob Lavee,[d] Salis Tager,[d] Erez Kachel,[d] Ehud Raanani,[d] Sergey Preisman,[e] Violete Glauber,[e] and Eran Segal[f]
[a]Bar-Ilan University, The Mina & Everard Goodman Faculty of Life-Sciences, Ramat-Gan, 52900 Israel
[b]CritiSense Ltd., Givat Shmuel, 54101 Israel
[c]Sheba Medical Center, Department of Vascular Surgery, Tel-Hashomer, 52621 Israel
[d]Sheba Medical Center, Department of Cardiac Surgery, Tel-Hashomer, 52621 Israel
[e]Sheba Medical Center, Departments of Anesthesiology and Intensive Care, Tel-Hashomer, 52621 Israel
[f]Assuta Medical Centers, Department of Anesthesia and Intensive Care, Tel-Aviv, Israel

Abstract. Background: The involvement of mitochondria in pathological states, such as neurodegenerative diseases, sepsis, stroke, and cancer, are well documented. Monitoring of nicotinamide adenine dinucleotide (NADH) fluorescence *in vivo* as an intracellular oxygen indicator was established in 1950 to 1970 by Britton Chance and collaborators. We use a multiparametric monitoring system enabling assessment of tissue vitality. In order to use this technology in clinical practice, the commercial developed device, the CritiView (CRV), is tested in animal models as well as in patients. Methods and Results: The new CRV enables the optical monitoring of four different parameters, representing the energy balance of various tissues *in vivo*. Mitochondrial NADH is measured by surface fluorometry/reflectometry. In addition, tissue microcirculatory blood flow, tissue reflectance and oxygenation are measured as well. The device is tested both *in vitro* and *in vivo* in a small animal model and in preliminary clinical trials in patients undergoing vascular or open heart surgery. In patients, the monitoring is started immediately after the insertion of a three-way Foley catheter (urine collection) to the patient and is stopped when the patient is discharged from the operating room. The results show that monitoring the urethral wall vitality provides information in correlation to the surgical procedure performed.
[DOI: 10.1117/1.3585674]

Keywords: biophotonics; biomedical optics; laser Doppler velocimetry; reflectometry.

Paper 11045R received Feb. 1, 2011; revised manuscript received Apr. 7, 2011; accepted for publication Apr. 8, 2011; published online Jun. 13, 2011.

1 Introduction

The need for a practical and simple medical device for *in vivo* monitoring of tissue energy metabolism in real time had stimulated many scientists as well as various medical device companies. Few companies and researchers had developed laser Doppler flow meters for tissue blood-flow monitoring,[1–4] tissue hemoglobin saturation levels (HbO_2),[5] tissue oxygen level (pO_2),[6] tissue CO_2 and pH[7] levels, and mitochondrial cytochrome oxidase redox state.[8] Nevertheless, none of the mentioned techniques is used in daily clinical practice in any medical field. The most important parameter to be evaluated is the balance between O_2 supply and demand defined as oxygen balance and represented by mitochondrial redox state. As of today, a number of measured parameters, in daily clinical practice, represent the integrity of the cardiovascular as well as respiratory system. In our previous publications,[9,10] we described few devices aiming to monitor tissue vitality using a single-point probe that measured up to four optical parameters from a small tissue area. These devices had never applied to routine clinical use due to factors such as size, price, or the ability to use and interpret the results as a clinical significant tool.

The new device described in the present paper was developed in order to overcome all the disadvantages of the early developed devices. During the research and development period, two models of the new multiparametric monitoring device were tested and submitted to the FDA for approval. The prototype of the CritiView (CRV), which was described few years ago,[9] was adapted to a single-point measurement in critical care medicine. The new model of the CRV enables one to integrate the measurements of three different locations of the tissue, thus improving the statistical basis of the measurement. Also, the new CRV is significantly smaller, thus enabling its incorporation into the small space available in operating rooms (ORs) or in intensive care units (ICUs).

1.1 *Patients Monitoring in Critical Care Medicine*

Cardiovascular insufficiency commonly occurs in critically ill patients and those undergoing major surgical procedures. The consequences of delayed recognition and treatment of circulatory shock prior to ischemic tissue injury can be irreversible. Patients undergoing a major surgery or hospitalized in the ICU frequently develop changes in systemic or peripheral hemodynamics. More than 20% of patients are expected to have acute cardiovascular dysfunction in the perioperative period of cardiac surgery.[11] Recently, Ospina-Tascon et al.[12] concluded, based on a literature survey, that "there is no broad evidence that any form of monitoring improve outcomes in the ICU and most

Address all correspondence to: Prof. Avraham Mayevsky, Faculty of Life-Sciences, Bar-Ilan University, Ramat-Gan, 52900 Israel; Tel: 972-35318218; Fax: 972-36354459; E-mail: mayevskya@gmail.com.

1083-3668/2011/16(6)/067004/21/$25.00 © 2011 SPIE

commonly used devices have not been evaluated by randomized controlled trails." Nevertheless, acute care practitioners are seeking new monitoring devices that would provide real-time data on the oxygen balance in patients at the tissue level.[13–15]

The pattern of the physiopathological event cascade that usually occurs in clinical conditions associated with an imbalance between oxygen delivery and oxygen consumption, under hypoperfusion-induced tissue hypoxia, is the common end product of circulatory shock. Various unstable metabolic states, infection, trauma. and surgical stress lead to metabolic disturbances and often result in cellular energy deterioration. The most common example of such a pathological state is sepsis, which is a major cause of death in critically ill patients.[16,17] The autonomic nervous system, mainly its sympathetic branch, including the adrenal gland, plays a major role in enacting the body compensatory mechanisms against a hemodynamic compromise The rapid compensatory reaction to hypovolemia, for example, includes redistribution of the blood flow to various organs, with a preferential blood flow to the most vital organs of the body, namely, the brain, heart, and adrenal glands,[18,19] while the peripheral organs or areas (the skin, gastrointestinal tract, and muscles), as well as other less vital visceral organs, undergo vasoconstriction and subsequent decrease in blood flow and O_2 supply.[20] This decrease in tissue perfusion could be detected by monitoring mitochondrial NADH in real time in those organs that experienced an early diversion of the blood flow.[21,22]

Currently, the monitoring of mitochondrial function in real time *in vivo* is not employed in clinical monitoring. Gastric tonometry and sublingual capnography have been used to assess tissue perfusion but have not yet been adopted for daily clinical use.[23–25] Tissue oxygen saturation measures have also been reported, but they can indicate decreasing values only at the end of a circulatory shock, not at its inception.

The effects of cardiopulmonary bypass (CPB) on cerebral cortical oxygenation during open heart surgery are well documented.[26] Cerebral hypoperfusion may also occur during the early postoperative period after cardiovascular surgery.[27] The monitoring of less vital organs (i.e., the skin or gastrointestinal tract) during cardiovascular surgery has been extensively reported.[28–30] In patients, the effects of hypothermic CPB on gut metabolism were an immediate decrease in blood flow followed by a recovery, while tissue oxygenation progressively declined after CPB.[31] Recently, Perner et al.[32] reported that, during CPB, lactate concentration in the rectal lumen increases, indicating a metabolic dysfunction of the rectal mucosa.

We tested the hypothesis that the urethral wall's mitochondrial function and microcirculatory blood flow in patients would be sensitive to macrocirculatory changes taking place during cardiovascular surgery. We chose this sample because of its existing invasive monitoring and the known alterations in the microcirculatory blood flow produced by surgery.

1.2 *Energy Metabolism in Mammalian Cells*

All cells in the body depend on a continuous supply of adenosine triphosphate (ATP) in order to perform their different physiological and biochemical activities. Figure 1 describes the basic processes occurring in a typical normal cell, using glucose as a major source of energy.

The breakdown of glucose into water and CO_2 includes two steps, namely, glycolysis (the anaerobic phase) taking place in the cytoplasm and oxidative phosphorylation (the aerobic phase) occurring in the mitochondria. Of the total yield of 38 ATP per

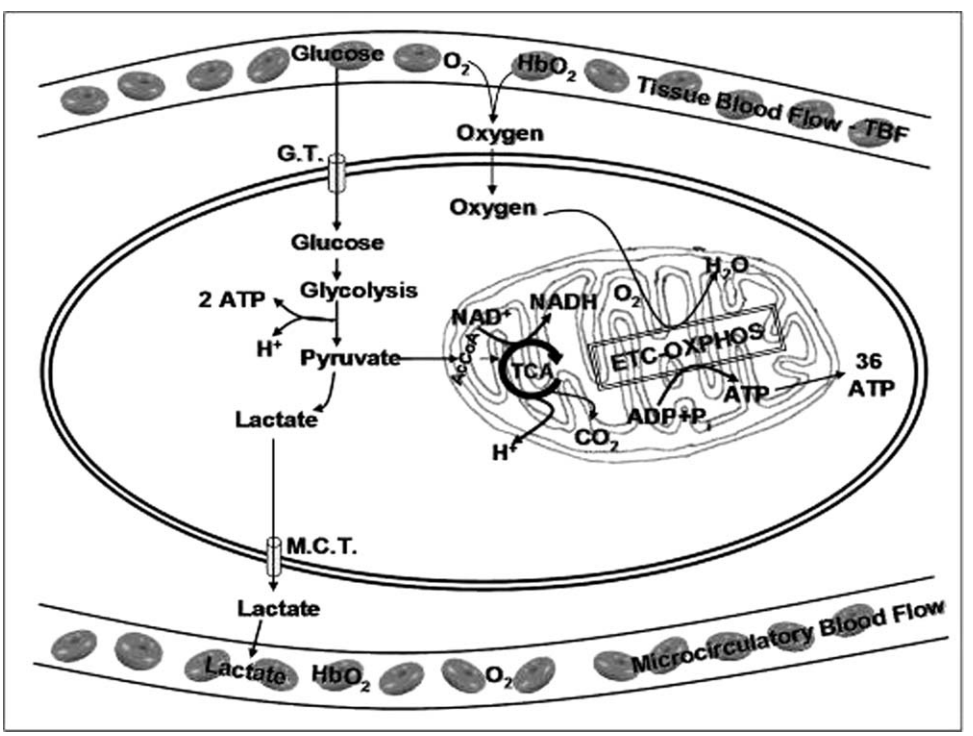

Fig. 1 Schematic presentation of tissue oxygen metabolism at the cellular and intramitochondrial level. GT, glucose transporter; MCT, monocarboxylase transporter; ETC; OXPHOS, oxidative phosphorylation; TCA; AcCoA, acetyl coenzyme A.

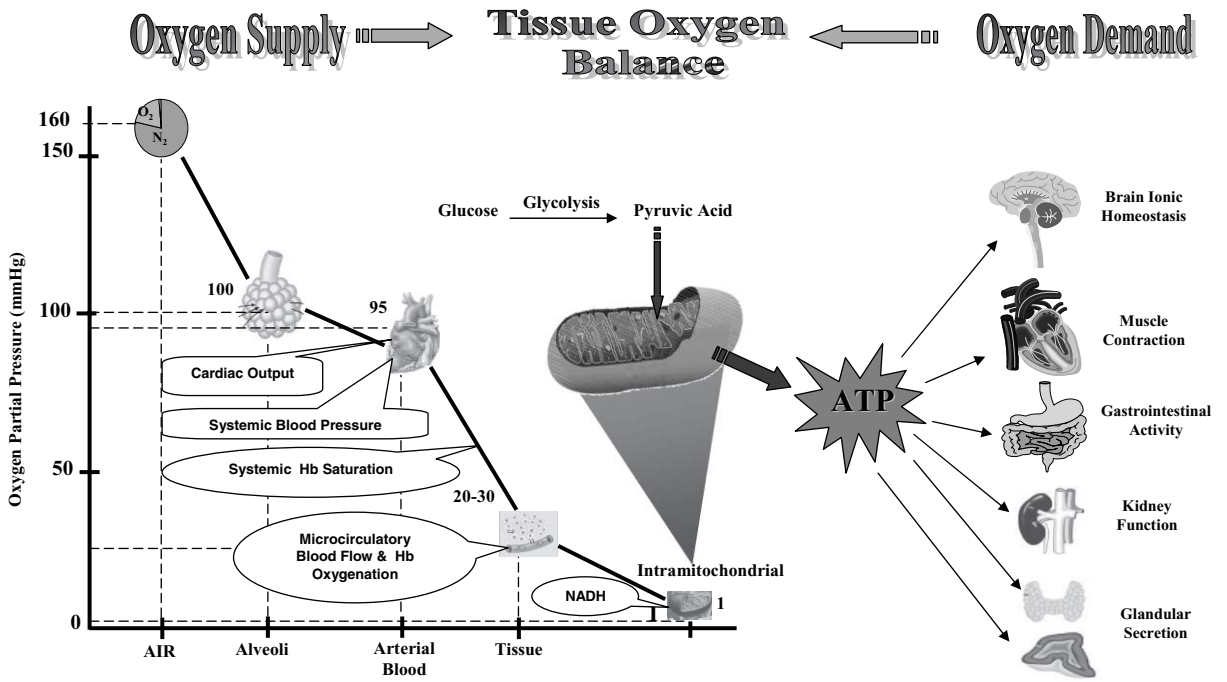

Fig. 2 Schematic presentation of the balance between oxygen supply and demand in a typical tissue. The supply is dependent on the availability of oxygen in the mitochondria, which is affected by the oxygen gradient between room air to the intracellular space (left side). The demand for energy is affected by the specific activities taking place in each organ.

mole of glucose, two are produced in the glycolysis process and 36 during the oxidative phosphorylation. It is important to note that oxygen availability in the mitochondrion is a critical factor for the normal ATP production in the cell. The exact level of oxygen inside the mitochondria *in vivo* is not well defined due to the inaccuracy of the measurement tools. It is evaluated to be ~1 mm Hg as compared to the high partial oxygen pressure, ~90 mmHg, existing in systemic circulation.[33] Glycolysis depends on the entrance of glucose from the capillary into the cell via the glucose transporter. The end product of glycolysis, pyruvate, is transported into the mitochondria by a specific carrier protein. The pyruvate is transformed, in the matrix of the mitochondria, into acetyl coenzyme A, which activates the tricarboxylic acid (TCA) cycle. In the absence of oxygen, the end product of pyruvate is lactate, which may leave the cell and pass into the microcirculatory blood stream via the monocarboxylase transporter located in the plasma membrane. In the mitochondria, the TCA cycle generates NADH (reduced nicotineamide adenine dinucleotide), which enters the electron transport chain (ETC) leading to the oxidative phosphorylation that generates ATP. The CO_2 released from the TCA cycle exits the cell as HCO_3^-, via the anion exchanger, into the blood stream. The continuous supply of oxygen to the mitochondria depends on two microcirculatory parameters: tissue blood flow (TBF) in the diffusible small vessels (small arterioles and capillaries) and the level of hemoglobin oxygenation or saturation (HbO_2) in the small vessels. Any change in the oxygen consumption by the mitochondria will be compensated either by downloading the extra oxygen needed from oxygenated hemoglobin or via an increase in the blood flow. Under a restriction of oxygen supply (hypoxia or ischemia), mitochondrial function will be inhibited and ATP production will decrease, while glycolysis will become stimulated. In most normal tissues and organs, this stimulation is not sufficient to provide the amount of ATP needed for the normal physiological and biochemical activities.

The pioneering work of Chance and collaborators, started in the early 1950s, ushered in a new era of studying mitochondrial function, in health and disease, using spectroscopic techniques.[34–36] The monitoring of NADH redox state in isolated mitochondria *in vitro*,[37] and later under *in vivo* conditions,[38] established the foundations for the understanding of cellular bioenergetics, under various pathophysiological conditions in experimental animals and patients.[39,40]

The functional capacity of a tissue is related to its ability to perform its work. It is possible to assess this ability through the knowledge of changes in the oxygen balance [i.e., the ratio of oxygen supply to oxygen demand in the tissue (Fig. 2)].

The electron transfers (oxidations/reductions) down the respiratory chain result in the production of ATP. Concomitantly with the electron transport, the respiratory chain components switch between reduced and oxidized states, each of which has different spectroscopic properties. Hydrolysis of the pyrophosphate bonds provides the energy necessary for the cell's work In order to assess the energy demand, it is necessary to measure different organ-specific parameters. In the brain, the energy demand can be evaluated by measuring the extracellular levels of K^+ that reflect the activity of the major ATP consumer Na^+/K^+ ATPase.[41,42] In the heart, most of the energy is consumed by muscle-contraction activity. On the other hand, the energy supply mechanism is the same in all tissues: oxygenated blood reaching the capillary bed releases O_2 that diffuses into the cells. Therefore, it is possible to evaluate tissue energy supply by monitoring the same four different parameters in all tissues, namely, mitochondrial function, tissue blood flow, volume, and

oxygenation. The intracellular level of mitochondrial NADH (the reduced form) is a parameter related to the tissue's state of energy metabolism. Energy exchange depends on pO_2 (partial oxygen pressure). Information regarding pO_2 in the tissue therefore is helpful for the evaluation of tissue metabolic activity. The sensitivity and accuracy of oxygen electrodes in the range of 1 mmHg is not sufficient for the evaluation of mitochondrial function.

The need for an intracellular pO_2 indicator, as a physiological and biochemical parameter of living tissue, emerged more than 50 years ago. Mitochondria are the intracellular organelles that consume most of the oxygen. Therefore, the redox state of electron carriers in isolated mitochondria *in vitro* as well as *in vivo* as a function of oxygen concentration has been extensively studied. Chance et al. concluded that "For a system at equilibrium, NADH is at the extreme low potential end of the chain, and this may be the oxygen indicator of choice in mitochondria and tissue as well."[43] Lubbers in 1995 concluded that "the most important intrinsic luminescence indicator is NADH, an enzyme of which the reaction is connected with tissue respiration and energy metabolism."[44]

Various parameters are measured in animal models or patients in order to evaluate the normality of the oxygen gradients ranging from 160 mm Hg in room air to ~1 mm Hg in the mitochondria as shown in Fig. 2. The respiratory function of the lungs is evaluated by measuring various parameters such as respiration rate and ventilation as well as levels of blood gases (pO_2, pCO_2 and pH). The second monitoring point along the oxygen gradient is the hemodynamic parameters of the cardiovascular system including cardiac output and systemic blood pressure. The next parameter is the saturation level of the arterial blood using the pulse oximetry. To date, the ability to measure tissue energy metabolism at the microcirculation and cellular level in clinical conditions is relatively limited.

1.2.1 *Monitoring of NADH: history, principles, and basic technology*

Since the discovery of pyridine nucleotides by Harden and Young,[45] more than 1000 papers have been published on the use of NADH as a marker for mitochondrial function. This type of research was started in 1955 by Chance & Williams[46,47] by defining the mitochondrial metabolic state in vitro. In order to understand mitochondrial function *in vivo* and under various pathophysiological conditions, it is important to monitor the redox state of the respiratory chain in real time

The discovery of the optical properties of NADH led to very intensive research since the early 1950s. The establishment of the method to monitor NADH *in vivo* was done between 1952 and 1962. An intensive use of the *in vivo* NADH monitoring approach began in 1962. The "classical" paper on in vivo monitoring of NADH was published in 1962 by Chance et al.[38] They were able to simultaneously monitor the brain and kidney of anesthetized rats using two microfluorometers. In 1962, Chance et al.[48] elaborated on this kind of in vivo monitoring and used it in other rat organs. The correction of the NADH fluorescence signal for changes in tissue absorption and scattering was initiated in the 1960s and 1970s by various investigators.[49–51] Most of the published material in this field of *in vivo* NADH monitoring of tissues used the subtraction of the reflectance signal (366 nm) from that of the NADH fluorescence signal measured to provide the corrected fluorescence signal.[52,53] A few attempts were made in order to improve the correction technique, but no significant improvement was found. In addition, the various correction techniques were listed and discussed in detail in Ince et al.[54] Most of the published material was based on a 1:1 ratio, when subtracting the 366-nm reflectance from the 450-nm fluorescence signal. We have found that subtracting the reflectance from the fluorescence or dividing fluorescence over reflectance provides similar net NADH changes. In 2006, Bradley and Thorniley[55] reviewed the available techniques for correction of fluorescence signals. They concluded, "even though research has been conducted into correction techniques for over thirty years, the development of a successful and practical correction technique remains a considerable challenge."

1.3 *Real-Time Monitoring of Tissue Vitality*

Several real-time invasive and noninvasive techniques have been developed to determine tissue energy metabolism or tissue vitality *in vivo*. A short description of the available techniques for monitoring tissue viability described by various investigators shown in Fig. 3 is presented here. These techniques could be adapted and used in experimental animals as well as in patients. In order to present the linkage between the systemic and tissue-level oxygenation, the pulse oximeter technique is also shown in Fig. 2; although the signal is not originated from the microcirculation.

1.3.1 *Systemic pulse oximetry*

This standard of care device is measuring the oxygenation level of the hemoglobin dependent on the pulse passing in the large arteries. In small vessels, the pulse disappears and, therefore, this technique cannot provide information on hemoglobin saturation in the microcirculation. Because of local changes in oxygen consumption, the systemic pulse may be relatively stable but the local Hb saturation may differ.

1.3.2 *Microcirculatory Hb oxygenation*

The level of oxygenated hemoglobin can be monitored at the microcirculatory level using the absorption spectrum of hemoglobin**,** which is different in its oxygenated or deoxygenated state. One possibility is to illuminate the tissue with light at the isosbestic wavelength point (not sensitive to the oxygenation level of hemoglobin), and a second wavelength, at a nonisosbestic point, in which the oxyhemoglobin absorbs more light than the deoxyhemoglobin form. By subtracting the two-wavelength reflectance, a parameter correlated to blood oxygenation level is obtained.[5,56]

1.3.3 *Microcirculatory blood flow*

Real-time monitoring of TBF can be achieved using laser Doppler flowmetry (LDF).[57–59] The LDF measures relative changes, which correlate with the relative TBF alterations. The principle of LDF is to measure the Doppler shift, namely, the frequency change undergone by the light reflected from moving red blood cells. The results are presented as percentages of a full scale (0–100%), providing relative perfusion values.

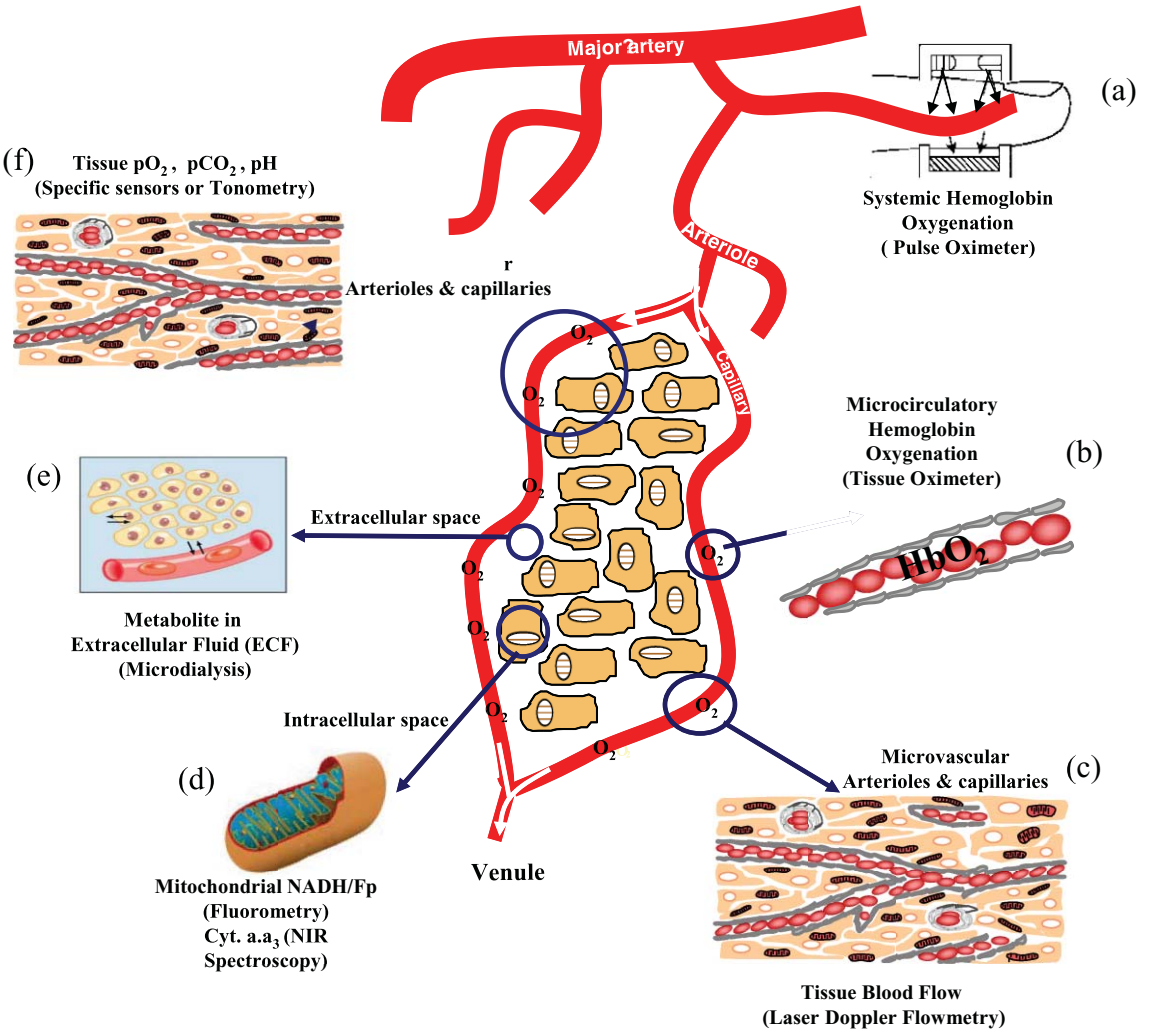

Fig. 3 The available techniques for real-time monitoring of energy metabolism at the tissue level. (a) The coupling between the macrocirculation monitored by the pulse oximeter and the microcirculation. (b–f) Monitoring of cellular and intracellular compartments (see text for details).

1.3.4 *Mitochondrial NADH/flavoproteins fluorometry and near-infrared spectroscopy*

NADH monitoring from the organ surface (brain, kidney, liver, testis, etc.) is performed by the fluorometric technique based on the original work by Chance and Williams.[46,47,60] The excitation light (366 nm) is passed from the fluorometer to the tissue through a bundle of quartz optical fibers. The emitted light (450 nm), together with the reflected light at the excitation wavelength, is transferred to the fluorometer through another bundle of fibers. The measured changes in fluorescence and reflectance signals are calculated as percent values relative to the calibrated signals under normoxic conditions. This type of calibration is not absolute but provides reliable and reproducible results for different animals and different laboratories.[41,42]

Monitoring of flavoprotein (Fp) fluorescence in blood-perfused organs *in vivo* is very problematic as compared to blood-free organs *in vitro*. Two factors affect the very weak fluorescence signal. Blood oxygenation and blood volume changes in the microcirculation induced artifacts in the measurements, which are very hard or impossible to be corrected.

Near-infrared spectroscopy (NIRS) is a noninvasive optical technique that evaluates the relationship between oxygen availability and consumption by monitoring of the oxidation-reduction state of cytochrome aa3 ($Cytaa_3$), although the artifacts of the hemoglobin signal in the $Cytaa_3$ signal remain problematic. Because tissue oxygenation is indicated by the state of cytochrome oxidase, the terminal enzyme of the respiratory chain, dynamic measurements of oxygen utilization, and perfusion can be achieved by NIRS.[61,62]

1.3.5 *Microdialysis*

The technique of tissue microdialysis allows continuous on-line monitoring of changes in tissue energy-related metabolites (e.g., glucose, lactate, pyruvate, adenosine, xanthine).[63] It involves the insertion of a catheter lined with a polyamide dialysis membrane into brain parenchyma that is perfused with a physiological solution (e.g., Ringer's lactate) at ultralow flow rates using a precision pump. Small molecules diffuse from the extracellular space into the perfusion fluid, which is then collected into vials that are changed every 10 to 60 min, allowing for

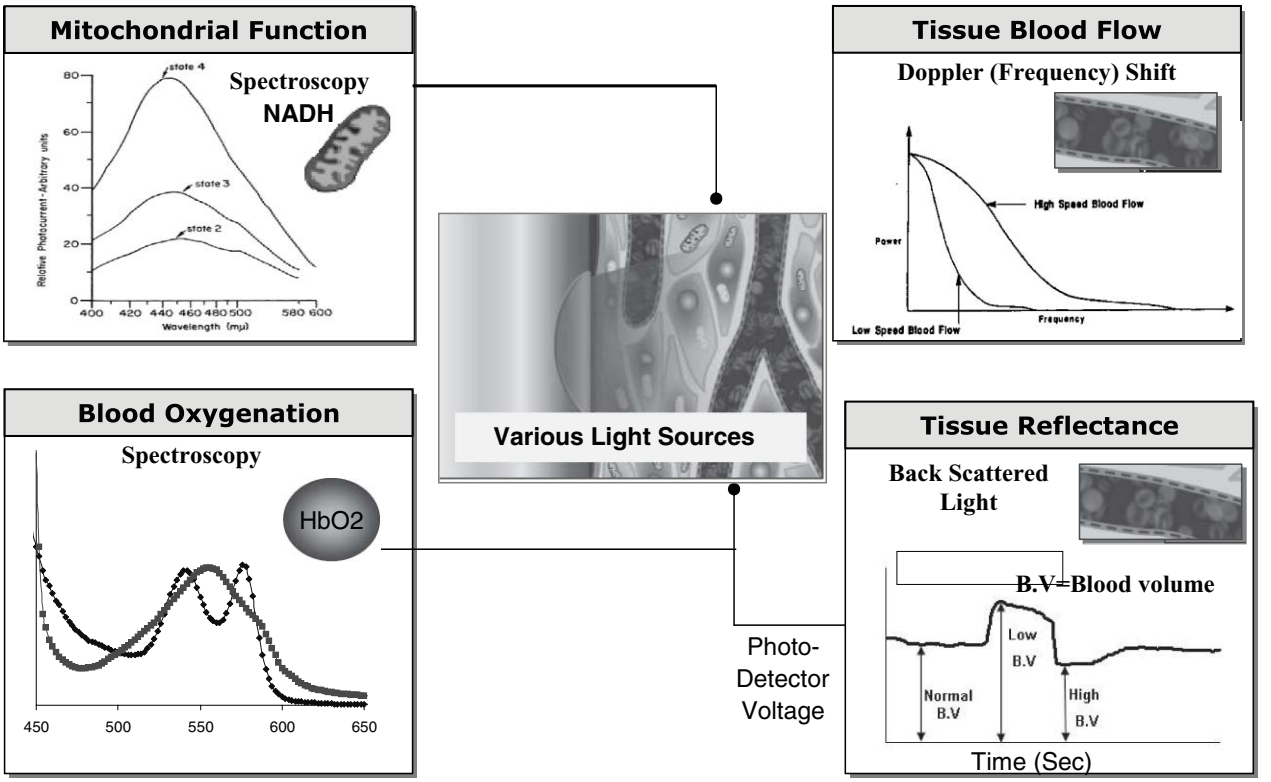

Fig. 4 Principles of tissue spectroscopy in order to evaluate tissue viability by the TVA and the CRV. Three of the parameters are monitored from the intravascular compartement while the NADH paramerer represents the function of the intramitochondrial space.

up to 70% equilibration across the dialysis membrane.[64,65] Cerebral microdialysis has great potential for exploring the pathophysiology of acute brain injury, drugs pharmacokinetics within the central nervous system, and responses to therapeutic interventions.

1.3.6 *Tissue pO_2, pCO_2, and pH*

Measurements of tissue pO_2, pCO_2, and pH are used as a monitoring modality in the neurosciences and critical care units,[66–68] and as a marker of tissue oxygenation in research protocols.[69–71] The technique involves the insertion of a microsensor into the brain parenchyma, either through a bolt inserted into the skull or directly through the craniotomy site and tunneled under the skin. At least two commercial microsensors allow direct, continuous measurement of brain tissue gases.[72]

The aims of this paper are as follows:

(1) To describe the principles and the technological aspects of tissue vitality optical monitoring.

(2) To present the upgraded technology of the CRV developed from the previous model of the CRV.[73] Also, the laboratory device, the tissue vitality analyzer (TVA), is presented.

(3) To compare the performance of the CRV and the TVA in animal models The TVA was used as a predicate device, namely, a device that the functions of the CRV were compared to the FDA regulation process. This comparison includes the *in vitro* and *in vivo* small animal experiments.

(4) To present preliminary clinical results obtained in critical care patients using the CRV.

2 Methodology

In the present study, the updated version of the CRV will be described and compared to the old laboratory monitoring system used in animal experiments named TVA. The two models of the CRV were cleared by the FDA. The first model was tested in small animal models (gerbils). The second model of the CRV was tested in small animals (gerbils), large animals (pigs), and in more than 30 patients. The TVA and CRV devices carries out certain *in vivo* spectroscopic measurements as a multiparametric monitoring device intended for the measurement of tissue in the metabolic state. The TVA consists of the combination of an NADH fluorometer, a laser Doppler flowmeter, as well as a reflectometer for the monitoring of microcirculatory blood oxygenation. The CRV is an integrated commercial unit that measures the same parameters. The two instruments are monitoring the following parameters (Fig. 4):

(1) Mitochondrial NADH fluorescence emitted at 420 –480 nm.

(2) Total backscattered light at the excitation wavelength reflected from the tissue. This parameter allows for correction of the NADH fluorescence measurement due to changes in tissue blood volume.

(3) Doppler-shifted laser light reflected from moving blood cells.

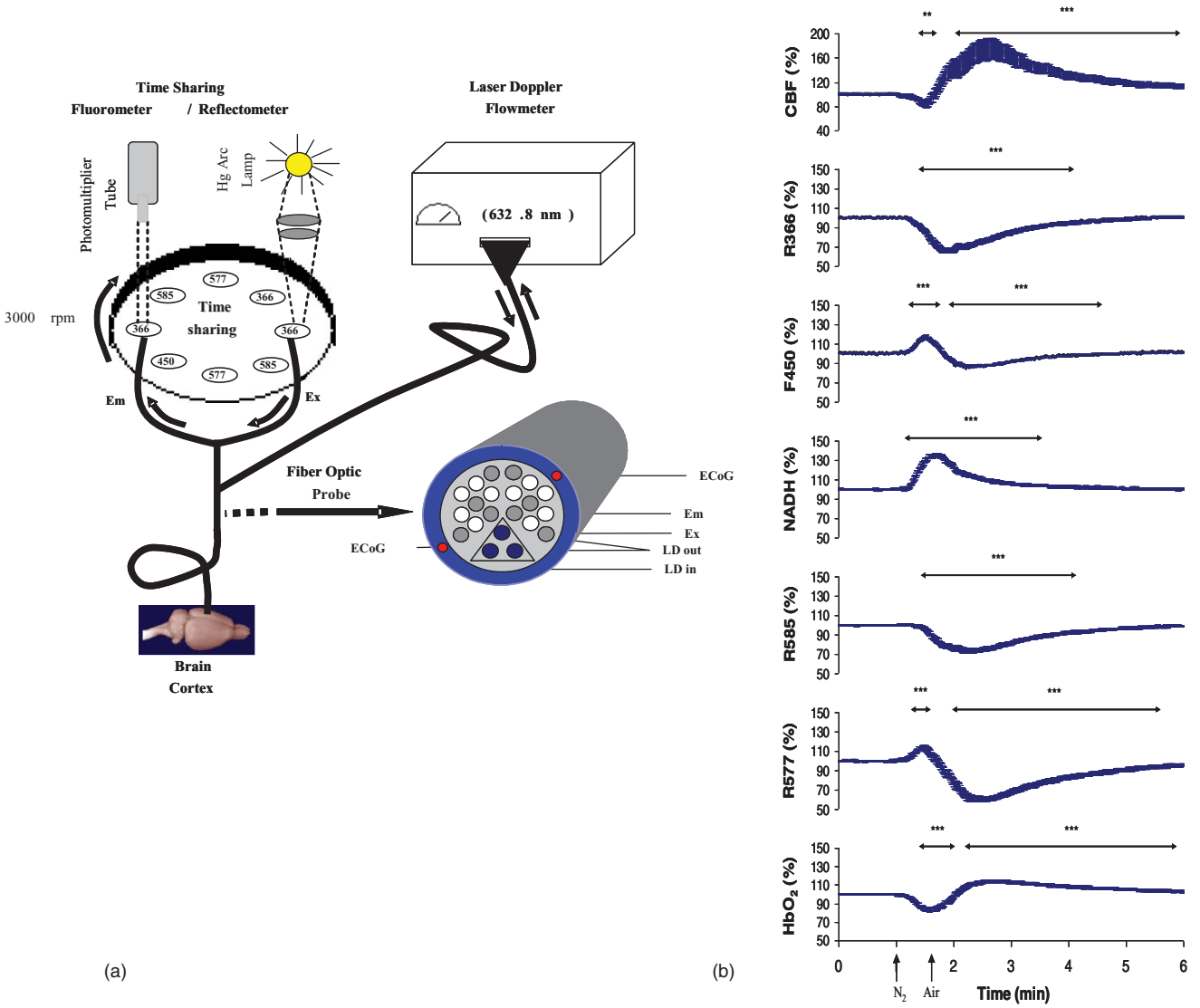

Fig. 5 (a) Schematic presentation of the TVA and (b) typical response to the lack of oxygen (anoxia). The details of the TVA components were described previously. TBF, tissue microcirculatory blood flow; R_{366}, reflected light at the excitation wavelength of NADH (366 nm); HbO_2, relative oxygenation level of hemoglobin.

(4) Two wavelength reflectometry enabling the monitoring of the saturation of HbO_2.

The TVA and CRV do not carry out the assessment of the monitored parameters. They simply provide the measured information to the user. These parameters contain information pertaining to the redox state of mitochondrial NADH of the tissue, microvascular blood flow and oxygenation in the tissue, and total blood volume of the tissue. Changes in these values reflect changes in the balance between oxygen supply and oxygen demand. Because the CRV is intended as an adjunctive measurement device when used in conjunction with conventional patient monitors, this further supports the low safety risk of the CRV. This means that the intensity of light in the various excitation wavelengths was below the level that may damage the tissue. The basic scientific principles of the TVA and CRV are identical, but the technology used is completely different.

2.1 *Tissue Vitality Analyzer*

In order to assess the hemodynamic and metabolic functions of the tissue, we used the TVA, which includes two devices: a time-sharing fluorometer-reflectometer for the mitochondrial NADH redox state and microcirculatory HbO_2 measurement[5] combined with a LDF for TBF monitoring [Fig. 5(a)]. The connection between the brain and the TVA was done by a flexible light guide. The fiber-optic probe includes fibers that were connected to the two instruments as shown in the enlargement of the bundle tip. The measurement of HbO_2, reflectance at 366 nm, and NADH were performed by the same excitation and emission fibers. The CBF was measured by three optical fibers located in the center of the time-sharing bundle of fibers. This system includes a rotating wheel with eight specific filters at the appropriate wavelengths (366 and 450 nm for NADH and 585 and 577 nm for oxyhemoglobin measurement) to four filters for excitation light and four filters for emitted light. The

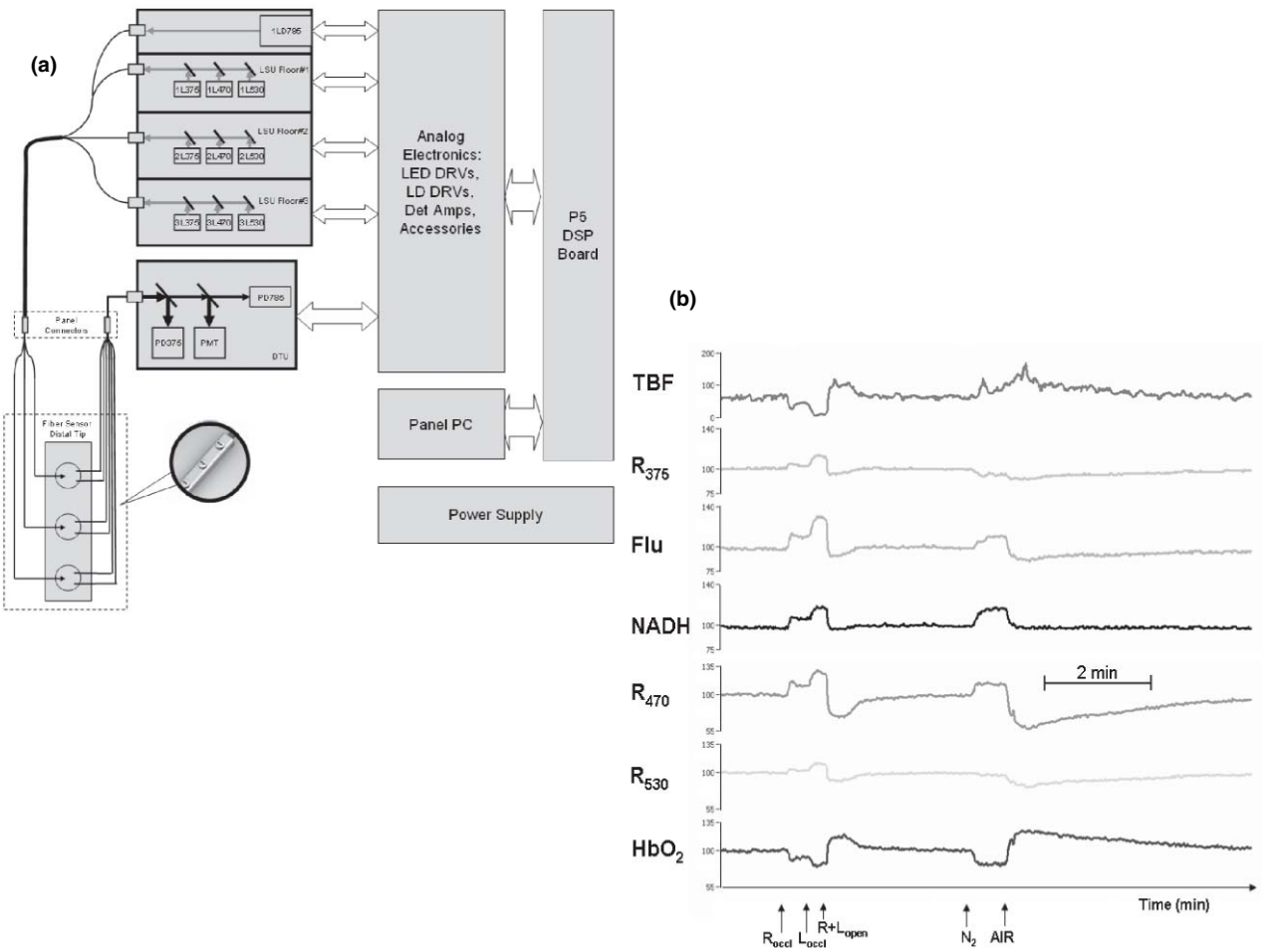

Fig. 6 (a) Schematic presentation of the CRV components. (b) Responses to ischemia and anoxia are presented. The effects of (left) ischemia and (right) anoxia on the four parameters measured from the brain of an anesthetized Gerbil. N_2, 100% nitrogen; R_{occl}, L_{occl}. occlusion of the right or left common carotid artery; $R + L_{open}$, reopening of the two carotid arteries.

wheel rotates at ~2400 rpm, which is a very high speed with respect to the kinetics of physiological changes; thus, NADH and oxyhemoglobin are simultaneously monitored.[5,39]

2.1.1 *Microcirculatory blood flow*

The optical fibers of the laser Doppler flowmeter were used for monitoring TBF. The LDF measures relative changes (in the 0–100% range), which are significantly correlated to the absolute values of TBF measured by other quantitative methods: H_2 clearance,[58] ^{14}C iodoantipyrine,[59] and radioactive microspheres.[74]

2.1.2 *NADH redox state fluorometer/reflectometer*

The principle of NADH monitoring from the tissue surface was described in Sec. 1.2.4. It is known that reflectance at 366 nm is inversely correlated to changes in the tissue blood volume;[5,39,75–78] therefore, the reflectance can be used as a hemodynamic parameter. The NADH fluorescence trace was corrected for hemodynamic artifacts by subtracting the reflectance signal (at 366 nm) from the fluorescence (450 nm) signal.[42,77] A detailed discussion about this issue can be found in our review articles.[39,41] The changes in the fluorescence and reflectance signals are calculated relative to the calibrated signals under normoxic conditions (100% NADH).[41,79–82]

2.1.3 *Hemoglobin oxygenation reflectometer*

Oxyhemoglobin measurement is based on the differences in the absorption properties of hemoglobin in its oxygenated versus deoxygenated states. The tissue is illuminated at two wavelengths: 585 and 577 nm. At 585 nm, oxyhemoglobin and deoxyhemoglobin have the same absorption characteristics (the isosbestic point); thus, the light emitted from the tissue reflects changes in tissue blood volume. At 577 nm, oxyhemoglobin has higher absorption ability (lower reflectance) than deoxyhemoglobin; thus, at this wavelength, the emitted light intensities are affected by the oxygenation levels as well as by the changes in blood volume at the measurement site. Therefore, subtracting changes in 585 nm reflectance from those at 577 nm provides a parameter correlated to net changes in blood oxygenation.[5,83]

2.2 *CritiView*

This new device, the CRV, is measuring the same four parameters as done by the TVA using different technology. In the mean time,

the FDA approved three out the four parameters. The HbO_2 will be submitted for clearance in the future.

2.2.1 *Light source unit*

The LSU [see Fig. 6(a)] of the CRV comprises a 785-nm continuous wave (cw) laser diode, which serves for laser Doppler measurement; a UV light-emitting diode [(LED), 375 nm] for NADH fluorescence excitation and for total back scatter (or reflection) measurement; and a blue LED (470 nm) and green LED (530 nm) for HbO_2. In order to enable a very high measurement dynamic range of fluorescence and reflection parameters, the light source unit is designed to enable a very wide range of the excitation intensities. To enable this wide excitation range and linearity, the system is designed according to a three-floors concept. Each floor comprises three LEDs: one UV LED with emission peak at 375 nm, one blue LED with emission peak at 470 nm, and one green LED with emission peak at 530 nm. The different wavelengths from all LEDs of the same floor are assembled together and coupled into a single fiber by a set of dichroic mirrors and appropriate collimation and focusing lenses. The current of each one of the discrete LEDs is set by the appropriate electronics drivers directly controlled by a digital to analog (D/A) of the digital signal processor (DSP). The difference between the floors is the output intensity. There is a high-, medium-, and low-intensity floors. The different excitation intensities are achieved by utilizing various pinholes while maintaining all other electro-optical properties as the same for all three floors. The light from all three floors and a laser diode is combined into single mixer fiber therefore enabling precise setting of the excitation intensity within a very wide excitation range. The NIR laser diode at 785 nm, for laser Doppler measurements, operates in cw operation mode. The UV LEDs, blue LEDs, and green LEDs operate in chopping mode. This enables usage of synchronous detection techniques in order to detect the NADH fluorescence and total backscatter light. Additionally, the chopping operation mode enables one to perform NADH measurements with very low excitation intensities well below the limits specified by the laser safety standards.

2.2.2 *Detection unit*

All six collection fibers of the fiber-optic probe are assembled into a single male SC optical connector. The light from the probe passes though the panel connector into a single thick optical fiber that delivers the light to the detection unit (DTU). At the DTU entrance, the collimation lens collimates the fiber output light. The collimated light is split according to the different wavelengths into the respective photodetectors by means of dichroic beam splitters. The first dichroic beam splitter reflects the total backscatter signal at 375 nm toward the photodiode detector. The higher wavelengths pass through the first beam splitter toward the second dichroic beam splitter. The second dichroic beam splitter reflects the NADH fluorescence signal at 450 nm and total backscatter signals at 470 and 530 nm toward the photomultiplier detector. Because of the chopping operation of the LEDs, the photomultiplier detector detects each one of the above-mentioned signals at different times (i.e., time-sharing operation detection mode). The second dichroic filter enables the laser Doppler signal at 785 nm to pass through it toward the photodiode detector. All acquired signals are digitized into the DSP by high-resolution 16-bit analog to digital (A/D).

2.2.3 *Digital signal processor*

The DSP is responsible for whole system control, initial data processing, and calculation of the Doppler parameter. The DSP is built around a Tern Inc. 586-Engine-P controller board with AMD SC520 CPU. After initial data processing, the calculated values are transmitted to the panel computer for final data processing display through RS-232 serial interface. The CRV device utilizes medical-grade main power supply for all electronic circuits, including the panel computer.

2.2.4 *CritiView optical probes*

Two types of fiber optic probes were developed for experimental animal and for clinical applications. (*i*) The pencil-style optical probe has one measurement point to be used on exposed tissue. The excitation and collection fibers are held together in a stainless steel element. It is comprised of one excitation fiber connected to respective excitation connector on the CRV panel and six collection fibers connected to the single collection connector on the CRV front panel. (*ii*) The Foley catheter optical probe for measuring the urethral wall vitality is based on a standard 3-lumen Foley catheter, which is an inflatable balloon retention-type catheter inserted through the urethra and used to drain the bladder. This probe construction enables the measurement of tissue metabolism at the urethral wall while draining urine from the bladder. The CRV Foley catheter optical probe is designed to perform optical measurements from three adjacent points on the tissue, 3.5-mm apart (Fig. 6). Each measurement point is comprised of one excitation fiber and two adjacent collection fibers. The three excitation fibers from the LSU are connected to the excitation connector on the CRV panel. All six collection fibers from the three measurement points are connected to the single collection connector on the CRV front panel. Figure 7 shows the finished probe inserted inside the three-way Foley catheter.

2.3 *Testing the CritiView In Vitro*

The aim of the study was to demonstrate the efficiency of the CRV device for the measurement of NADH concentration. The experimental methodology is straightforward. Various solutions of NADH were measured with the CRV. Insofar as the measurement with the CRV involves placing its probe tip into the solution, one might ask if this measurement is the same as placing the tip of the probe against a tissue surface. The equivalence of these two measurements can be understood if one considers that, although immersion in aqueous solution and placement adjacent to tissue are, clearly, two different physical situations, nevertheless, the process and principle of measurement that takes place is the same for both. Aside from their contiguity, there is no interaction between the probe and the solution or any adjacent tissue. The probe merely collects emitted light from its immediate environment (i.e., a hemispherical volume adjacent to the probe tip) and transfers the collected light to detectors for measurement Therefore, for the purposes of comparison of CRV spectroscopic characteristics to those of control NADH solution and to a clinical fluorometer, the CRV probe can be positioned on

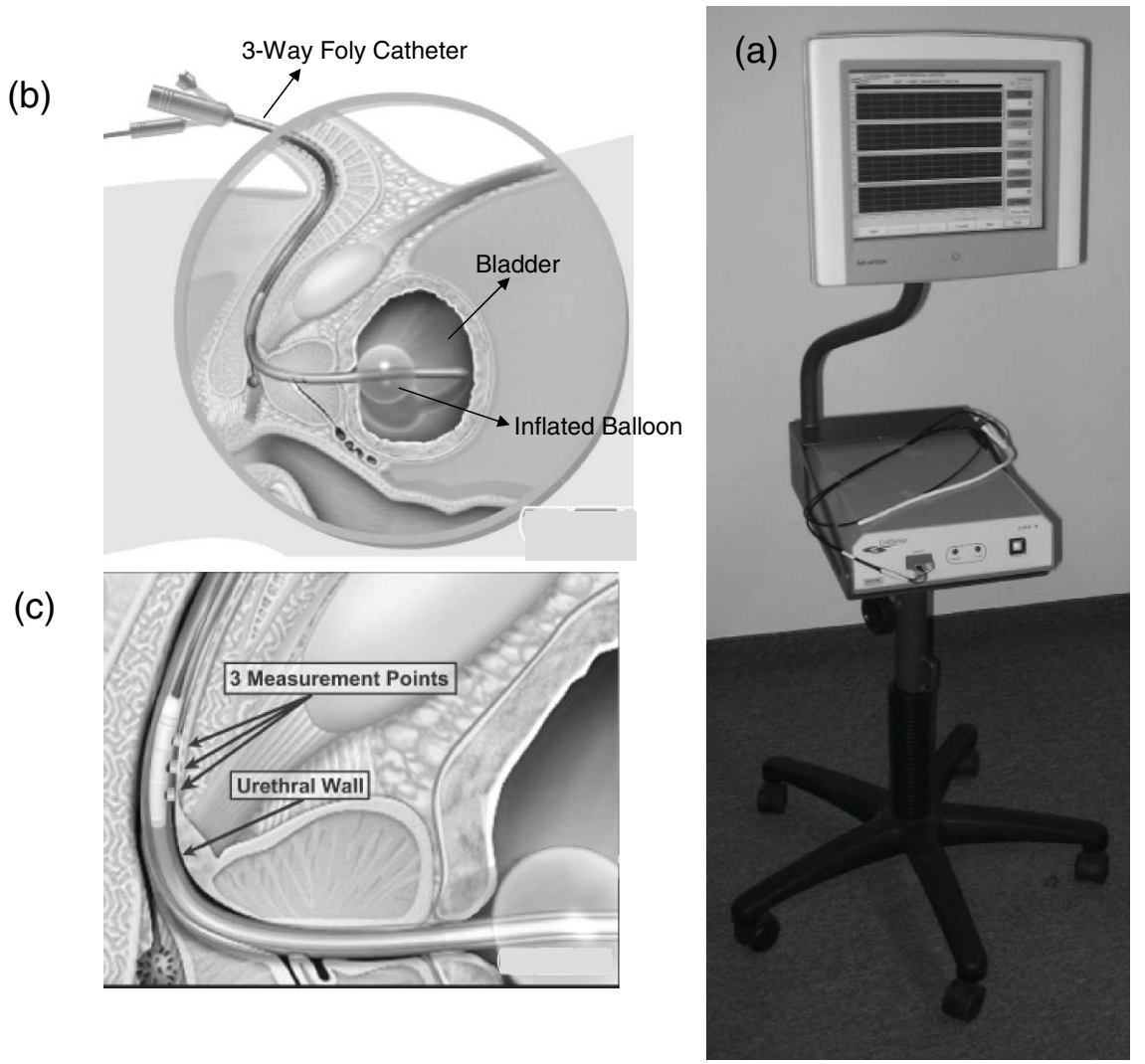

Fig. 7 (a) The CritiView device used in the present study and (b,c) location of the three-way Foley catheter and the monitoring sites in the urethral wall.

the surface of a tissue or a liquid, or it can be inserted into the tissue or liquid. Three sets of solutions with known concentrations of NADH and double distilled water (DDW) were prepared in the following way: Stock solution of 1 mM NADH was prepared by dissolving 14.188 mg NADH in 20-ml DDW. The samples of NADH solutions (5 ml) were prepared in glass vials by the appropriate dilution of the stock solution with DDW, which also used a blank that was subtracted from the actual reading made by the CRV. The "pencil-type" probe of the CRV was placed in the vials for 10 s, and a reading was taken. The probe was taken out of the solution, and a second reading was recorded. This was repeated again so that three readings were averaged. A second and third set of diluted solution were prepared by the same procedure and were measured in the same way. The same procedure was used with the predicate CritiView-CRV1 with onset of NADH solutions.

2.4 *Testing the CritiView in Animals*

The aim of this study and report is to describe, in detail, the *in vivo* control study of the CRV device in order to demonstrate substantial equivalence to its predicate device. As mentioned before, the original animal laboratory device was the TVA. This device was used in our lab for a number of years before the development of the commercial devices: the CRV or the two models of the CritiView. Each one of the three devices was tested in animal experiments in order to verify the performance of the device by itself. After this testing, the TVA was used as a predicate device for the newly developed CRV. The first CRV was compared to the TVA, and the second CRV was compared to the first CRV. In this report, we are presenting the comparison between the TVA and the first CRV. Basically, the comparison between the two CRV models were submitted to the FDA but are not presented here. The performance of the CRV device in measurement of changes in TBF NADH fluorescence, tissue reflectance, and HbO_2 resulting from standard metabolic perturbations in an animal model (gerbils) was done. All signals are monitored by the CRV as relative values. This brings all the calculations to be presented as "percent change of the signals." The TBF outputs of the CRV are curves of signal measurements as functions of time. In order to assess the performance of CRV and the TVA in measurement of TBF, we performed a series of

experiments in which the TBF of animals was measured simultaneously by the two instruments. The same basis was applied to the other three parameters, namely, NADH, reflectance, and HbO_2 in the same statistical analysis principles. The response time of the different devices was the same (3 s). The purpose of the statistical analysis is to demonstrate that the two curves of each experiment are equivalent. Because the scales of the instruments are not identical, it is meaningless to compute the difference between the two curves. In fact, equivalence in this case means "having the same direction of change." That is, when one curve goes up, the other goes up, and when one goes down, the other goes down. The appropriate statistical measure for such behavior is the correlation coefficient that uses a large number of data points collected by each instrument in every episode. It is desirable to have a correlation coefficient as close to $+1$ as possible between every pair of corresponding curves. Thus, by computing correlation coefficients between two curves, it is possible to measure the statistical equivalence between them.

2.4.1 *Animal preparation*

In order to test the depth of anesthesia in each gerbil monitored, we used a surrogate systemic parameter that represents the function and the intactness of the cardiovascular and respiratory systems. The parameter is the level of the hemoglobin oxygenation in the systemic blood, SpO_2 measured by a standard veterinary pulse oximeter suitable for small animal experiments (model 8600V, Nonin Medical Inc., Minneapolis, Minnesota) The SpO_2 was very high and stable during the entire period of monitoring. During the four perturbations imposed on the gerbil, a clear decrease of the SpO_2 was recorded. This decrease in SpO_2 during anoxia, hypoxia, and terminal anoxia is according to the availability of oxygen to the body. The decrease in SpO_2 during cerebral ischemia is probably due to stimulation of the sympathetic and parasympathetic nerves that are affected by the pulling of the carotid arteries during the ischemic episode.

2.4.2 *Operation procedure*

Male rats (250–300 gr) and mongolian gerbils (50–75 gr) were used. We had operated 35 rats and 25 gerbils that were used for the various in vivo studies. This includes the testing of the various devices as well as the comparison studies between the TVA and the CRV. The animals were anesthetized by Equithesin (E-th = chloral hydrate 42.51 mg; magnesium sulfate 21.25 mg; alcohol 11.5%; propylene glycol 44.34%; pentobarbital 9.72 mg) intraperitoneal (IP) injection of 0.3 ml/100 g body weight. The animals were kept anesthetized during the operation, and during the entire monitoring period, by additional IP injections of E-th 0.03 ml in gerbils and 0.1 ml in rats, every 30 min. The addition of small volumes of E-th every 30 min kept the animals in a stable state. In the gerbils, the two common carotid arteries were isolated just before brain surgery and ligatures of 4–0 silk thread were placed around them. The animal was placed in a head holder in the supine position. After a midline incision of the skin, an appropriate elliptic hole (about 3×8 mm) was drilled in the parietal bone of the right hemisphere. The dura mater remained intact, and a light guide holder—cannula—was placed in the drilled hole, and extra pressure on the tissue was avoided. Two stainless steel screws in the left parietal bone were used to fix the cannula, with dental acrylic cement. Body temperature was measured by a rectal probe (Yellow Springs Instrument, Yellow Springs, Ohio) and was regulated to be at the range of 35–37°C using a heating blanket.

2.4.3 *Metabolic perturbations*

Anoxia. Exposure of the animal to oxygen deficient atmosphere by spontaneous breathing of 100% N_2, for a period of time ($\sim$25 s) until changes are observed on the monitor and the animal has stopped breathing. The animal is then allowed to breathe normal room air by spontaneous breathing or by short artificial respiration.
Ischemia: Reversible occlusion (30 s) of the two common carotid arteries by constricting them with threads.
Hypoxia: Exposure of the animal to spontaneous breathing of low oxygen concentration (6% oxygen in air) for a short period of time (60 s). The animal is then allowed to breathe normal room air by spontaneous breathing.
Terminal Anoxia: Exposure of the animal to complete irreversible anoxia by exposing the animal to 100% N_2 until the death of the gerbil.

The application of the various gases was done by placing a small tube, connected to the gas cylinder, around the nose of the animals. The flow of the gas was very slow (<1 l/min) in order to avoid respiratory disturbances.

2.4.4 *Experimental protocol*

Monitoring the various parameters was started immediately after the end of operation. This was done by using two needle-type optical probes connected to the CRV and the CritiView-CRV1 and placed inside the cannula cemented to the skull. In order to check the intactness and the physiological status of the brain, a 20-s anoxia was induced. Rats and gerbils that present abnormal response were discarded before running the experimental protocol. In each monitoring system, the variation in the response to short anoxia was in the range of $\sim$10%. For example, if the increase in NADH was in the range of 50–60%, any animal that showed 20–30% or 70–80% was not involved in the study and discarded at this stage of the study. Normally, only 5–10% of the operated animals were discarded at this stage. When body temperature reached the range of 35–37°C, the exposure of the animals to the various perturbations started. The animals were exposed to the various conditions having an interval of $\sim$10 min between each test to allow recovery. The pulse oximeter value was used in order to assure the complete recovery. The data were collected at a rate of one sample per second and stored in different channels of a computerized data acquisition program.

2.5 *Testing the CritiView in Patients*

All patients included in the clinical testing signed an informed consent form after the approval of the protocols by the Helsinki committee of Sheba Medical Center, Israel. Using the CRV [Fig. 7(a)], we studied three groups of human subjects. The first group included general ICU patients ($N = 15$) monitored consecutively (Sheba Medical Center). During this period, we defined and improved the dynamic range of the monitored parameters and adjusted the tissue optical characteristics for the

Table 1 List of surgical procedures in cardiovascular patients.

1. Anesthesia
2. Inserting of Foley catheter and beginning of monitoring
3. Skin cut and chest opening
4. 4 Hypothermia (optional)
5. Isolation of a. Mammary artery(ies)
b.Vein(s)
6. Preparation of large blood vessels (aorta and vena cava)
7. Connecting the patient to HLM or pump off procedures
8. Surgical procedures: a. Aortic valve or aneurysm repair
b. Heart valve's treatment or replacement
c. CABG
9. Gradual Recovery to the beating heart
10. Closing of chest and skin
11. Disconnection of Critisense's CRV unit
12. Duration of monitoring period, 2–8 h

human urethra, which were assumed to be different from those of the gerbil brain. The data obtained from these patients proved that the Foley catheter, shown in Figs. 7(b) and 7(c), provided appropriate monitoring during at least the first five days after its insertion in the patient. The second group included five patients undergoing abdominal aortic aneurysm repair, where a defined period of aortic cross-clamping was needed for the surgical repair. The third group included 20 patients undergoing cardiac surgery, 18 of which required cardio-pulmonary bypass for 1–2 h. In the last group of patients, the hypothesis was as follows. The chest opening and connection of a patient to the heart and lung machine may develop body metabolic instability and negative oxygen balance even though the machine should provide the needs for oxygen. The objective was to test the CRV in an extreme, controlled event and to evaluate the responses during the entire operation period.

The protocol included the monitoring of CritiView parameters starting immediately after insertion of the three-way Foley catheter until the end of the operation procedure in the OR. The monitoring period included the following steps: opening of chest, vascular and heart procedures, body perfusion by heart and lung machine (HLM), and recovery to the beating heart. The details of the operation procedure are presented in Table 1.

2.6 *Statistical Analysis*

In Sec. 3, we present the data as mean and standard error of the mean. We preferred this presentation because most of the physiological journals prefer this approach. In any case, this presentation mode is not affecting the calculation of the significance level. Various statistical tests were used in the present study. For the *in vitro* testing, regression analysis was performed. For the *in vivo* monitoring data analysis, the analysis of variance (ANOVA) test was used. The effects of surgery stages on the tissue microcirculatory blood flow level were analyzed using repeated measures ANOVA (GLM procedure of SPSS 15.0). For the analysis of patients in the third group, we used repeated measures ANOVA, sphericity assumed ($F_{2,20} = 11.170, p = 0.001$). The pairwise comparison (Bonferroni comparison) was utilized.

3 Results

3.1 *Bench Tests and Stability*

Bench test data are presented in Fig. 8(a). Three regression lines, related to the three sets of measurements, were calculated and found to be highly statistically significant. As seen, the CRV is measuring the NADH accurately. In Fig. 8(b), the stability of the microcirculatory blood flow and NADH for the brain and small intestine are shown. In terms of calculated stability, the values found for the microcirculatory blood flow were better than 2% per hour and for the other parameters were $<1\%$.

3.2 *Small Animals (Rats and Gerbil Brain)*

The two monitoring systems were tested *in vivo* in the rat and gerbil brain, and typical results are shown in Figs. 5 (TVA) and 6 (CRV). Figure 5(b) shows the responses of the brain to anoxia (100% nitrogen) measured by the TVA in a rat. As can be seen, the negative correlation between HbO_2 and NADH are very clear due to the decrease in the lack of oxygen. The microcirculatory blood flow, measured by the LDF, shows an initial decrease followed by long-lasting overshoot (hyperemia). Also, the changes in the two reflectance signals (R366 and R585) are very similar under anoxia. Figure 6(b) presents the responses of tissue microcirculatory blood flow, reflectance (R_{375}), NADH, and HbO_2 measured by the CRV. Responses to ischemia (left) were induced in two steps: the occlusion of one carotid artery (R_{occl}) followed by the occlusion of the second artery (L_{occl}). A pronounced decrease in HbO_2 strongly correlated with an increase in NADH. Insignificant recovery was noted shortly after the unilateral occlusion, presumably due to microcirculatory blood-flow compensation through the anterior part of the circle of Willis. Hyperemia was noted in the TBF and HbO_2 but not in the NADH traces after the reopening of the carotid arteries. The time needed for recovery to the baseline value is much shorter for the NADH signal as compared to the TBF and HbO_2 signals. As seen in Fig. 6(b), under anoxia (100% N_2), the decrease in HbO_2 was followed by an increase in NADH. The TBF showed a later increase that turned into a hyperemic response that was also recorded in the HbO_2 signal after recovery from the anoxia. In order to compare the performance of the two devices, namely, the TVA and CRV, an appropriate number of animal experiments were performed. We used four perturbations in each animal and compared the responses of the four parameters. Typical results of those experiments are shown in Fig. 9. The two instruments were connected to the same brain of a gerbil, and the responses to various perturbations described in Sec. 2 were recorded. In the center of Fig. 9, the wavelengths used in the two instruments to measure the four parameters are shown. In our previous

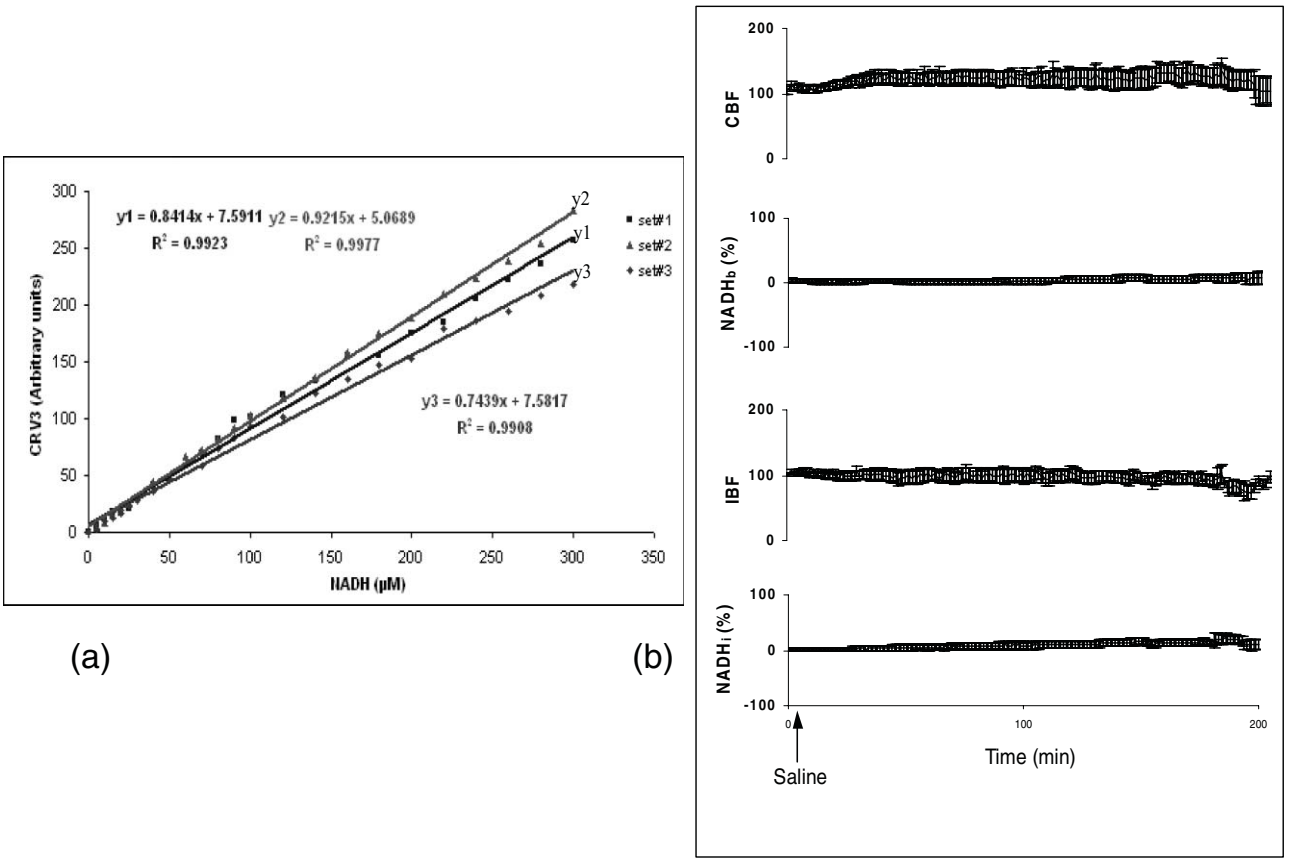

Fig. 8 (a) Fluorescence readings (three sets) of the CritiView plotted against NADH concentration after subtracting the reading of the blank solution. A linear regression was calculated, and the equation and R^2 are presented for the three sets of control solutions. (b) The stability for 200 min of the monitored parameters in two organs. The upper two traces were measured from the brain, while the other two are from the small intestine.

studies, we were able to compare four monitored sites in the brain by using the multisite monitoring system.[42] The responses to anoxia in all sites were very similar; although a different location was monitored. The main reason for this similarity is that the relatively large monitored site (>1 mm diam) is integrating a large number of cells and vascular components that provide similar responses. Therefore, we used this approach to test the equivalency of the two instruments.

As can be seen, the responses to anoxia recorded by the two instruments were very similar in this typical animal. Statistical analysis of the group of at least 10 animals showed a significant correlation between the two responses of all four parameters measured. The total number of episodes used for the statistical analysis was 12 for TBF, 22 for NADH, 16 for reflectance, and 17 for HbO_2. The statistical analysis of entire episodes were done and found to be significant. Because of space limitations, the details are not presented here.

3.3 *Human Studies*

3.3.1 *Patients in the intensive care unit*

Three responses measured in ICU patients are shown in Fig. 10. We assumed that, under stressful situations, in a less vital organ (such as the urethral wall) the microcirculatory blood flow will be reduced and oxygen delivery to the mitochondria will diminish. In a female patient [Fig. 10(a)], the responses to a cessation of spontaneous respiration were recorded. As seen, a clear hypoperfusion was recorded in the urethral wall together with a significant increase in NADH levels. As soon as artificial ventilation was restarted, the signals returned to baseline levels. In another patient, a dramatic decrease in the urethral wall energy state was recorded during a standard airway-suction procedure. As Fig. 10(b) shows, a large decrease in the microcirculatory blood flow was measured simultaneously with a marked increase in NADH. These changes suggest that the cardiorespiratory stressful situation induced by suction could be detected by the decrease in the urethral wall viability.

The third patient was monitored during the early postoperative period after coronary artery bypass graft (CABG) operation [Fig. 10(c)]. The left side of Fig. 10(c) shows that, during the initial 3 h of monitoring, the NADH levels were relatively stable ($\pm$20% change). During the next 40 min of monitoring [right side of Fig. 10(c)], a marked mitochondrial dysfunction was recorded (100% increase in NADH) in parallel to a decrease in TBF. The NADH response included two types of change, namely, a pronounced continuous increase in the NADH levels as well as a number of transient elevations lasting 1–5 min each. It was found that, during this period, a cardiac tamponade was developed and the patient was returned to the operating room for resternotomy. The hemodynamic parameters (heart rate and blood pressure), shown in the boxes below

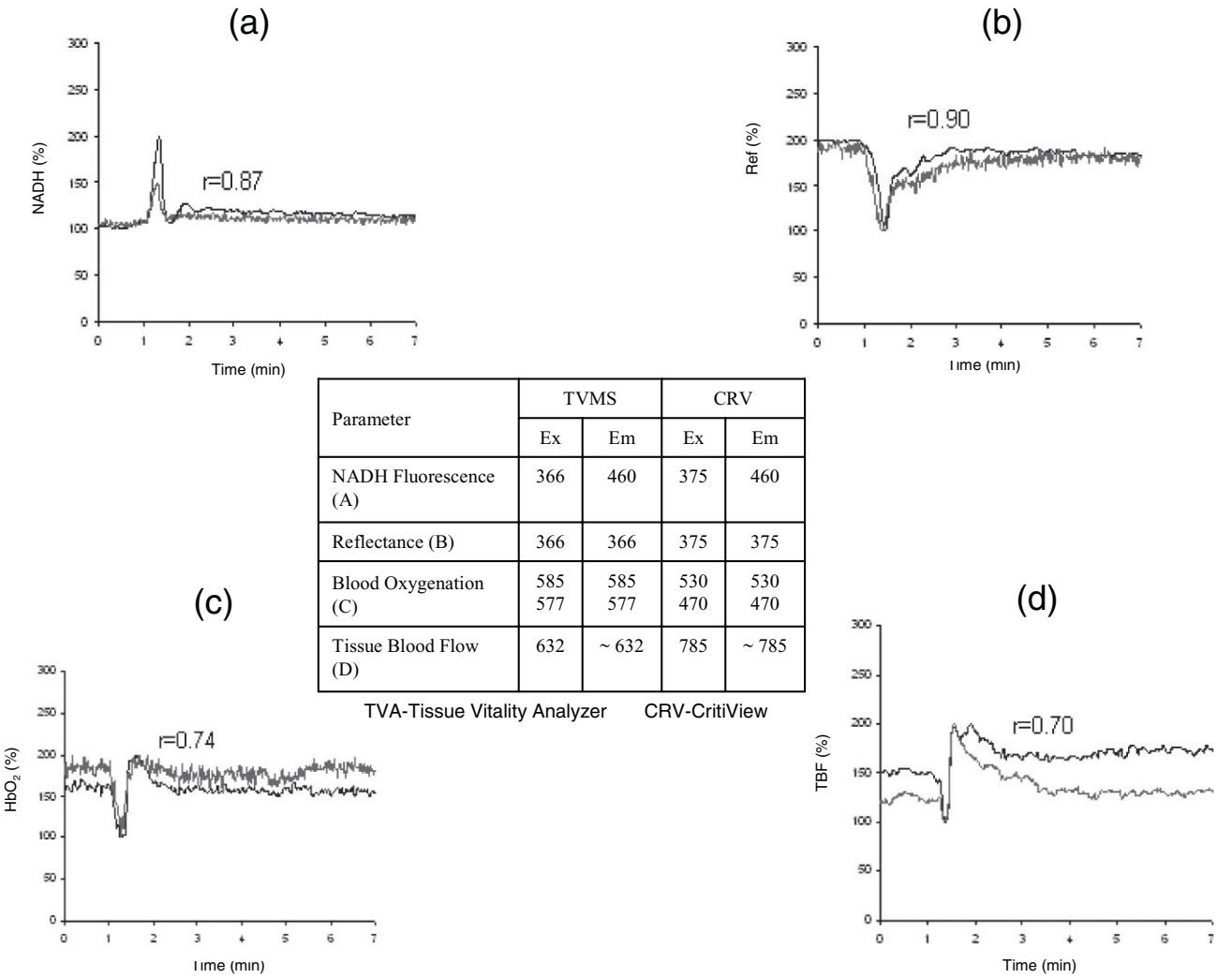

Parameter	TVMS		CRV	
	Ex	Em	Ex	Em
NADH Fluorescence (A)	366	460	375	460
Reflectance (B)	366	366	375	375
Blood Oxygenation (C)	585 577	585 577	530 470	530 470
Tissue Blood Flow (D)	632	~ 632	785	~ 785

TVA-Tissue Vitality Analyzer CRV-CritiView

Fig. 9 Comparison between the responses to anoxia measured by the TVA and CRV in the gerbil brain. In each of the four pictures, the two lines represent the results obtained by the two devices. In the center area, the various wavelengths used in the two devices are shown.

Fig. 10, were not clearly correlated to the development of the tamponade.

3.3.2 *Patients undergoing open repair of abdominal aortic aneurysm*

In five patients, clear but not entirely consistent responses to the clamping of the abdominal aorta were observed and recorded. During this phase of the operation, the microcirculatory blood flow in the urethra decreased in all patients, while the results of NADH measurements showed some variability. Typical responses to aortic occlusion in one of the abdominal aortic aneurysm (AAA) patients are shown in Fig. 11(a). The preparation of the aorta for the clamping procedure (marked as A) led to a clear transient decrease in TBF, as well as an increase in the NADH level. The clamping of the aorta led to a maximal decrease in TBF in parallel to the increase in NADH. In this patient, the monitored HbO_2 showed a clear decrease during the clamping interval. Because of a decrease in tissue blood volume, during the aortic occlusion, the reflectance trace showed a large increase until the reopening of the occluded aorta. Immediately after declamping, the initial small increase in TBF led to a fast recovery of the HbO_2 and NADH redox state. All signals recovered to the same values measured during the short control period; although, the occlusion interval lasted for >80 min. In Fig. 11(b), the typical correlation between the various parameters is presented. Data were extracted from the five patients of this group according to the six stages of the operation: Stage 1, 10 min before the clamp; stage 2, 10 min after the clamp; stage 3, midpoint of the clamping period; stage 4, 10 min before the declamp; stage 5,- 10 min after the declamp; and stage 6, the last 5 min of monitoring in the OR.

The results for the five patients [Fig. 11(c)] showed a pronounced decline in the mean TBF values, noted in our experiments from the second stage of the surgery up to the fourth stage. The dependence of TBF on time was statistically significant. The difference was significant for all stages of surgery (t1–t4, $p = 0.004$), but was non-significant ($p > 0.05$) for the partial intervals (t2–t3 and t3–t4). This analysis indicates that the only statistically significant change is between points

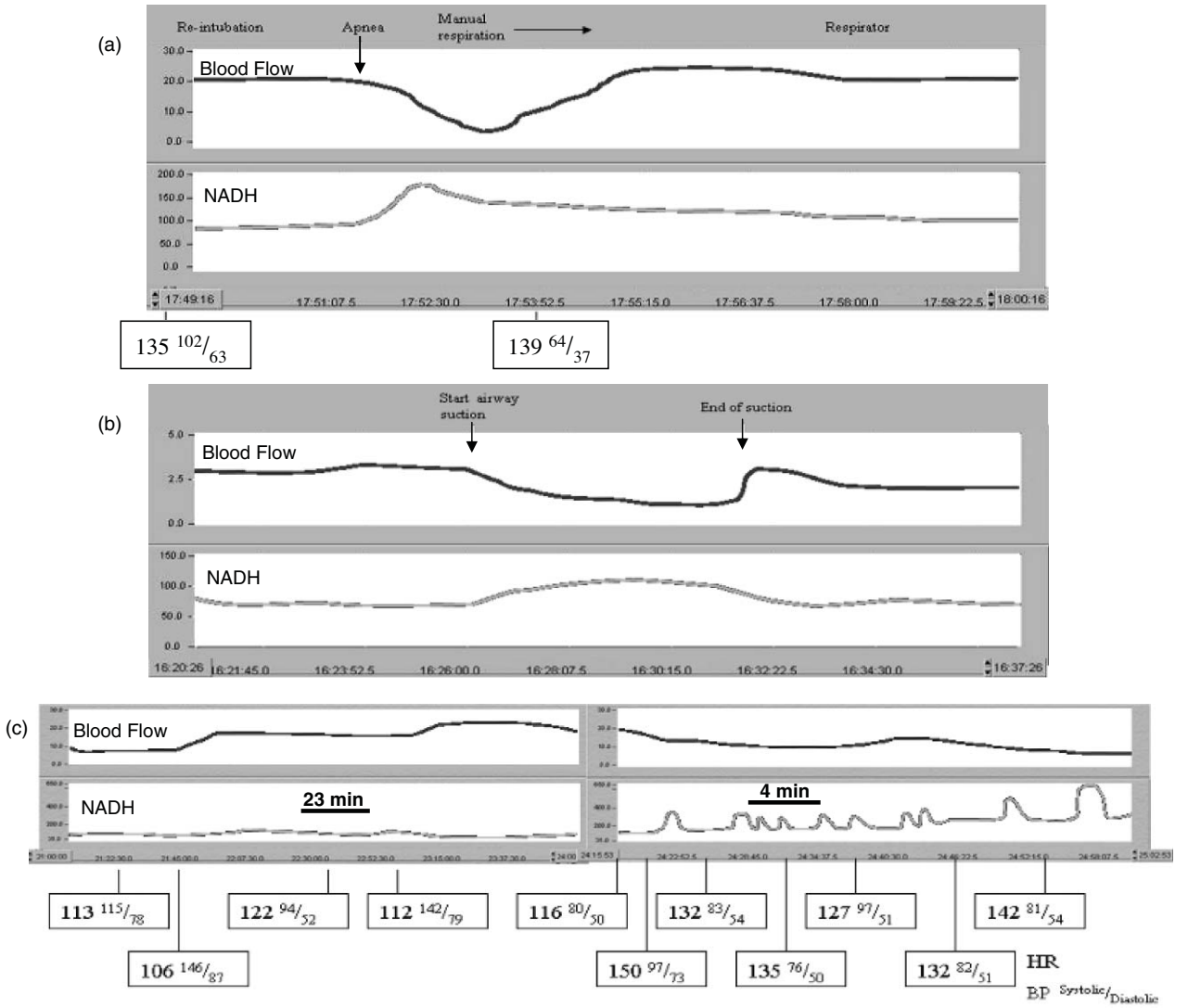

Fig. 10 The results of three patients monitored in the ICU using an early version of the device named the tissue spectroscope: (a) Responses to a cessation of spontaneous respiration in a female patient, (b) effects of the standard airway suction procedure on the viability of the urethral wall, and (c) monitoring of a patient in the cardiac ICU during the initial 4 h after the bypass surgery, showing the development of cardiac tamponade.

1 and 4. The changes in the NADH level were significant only when the basal level (t1) was compared to t3.

3.3.3 *Patients undergoing open heart surgery*

Thirteen patients underwent a coronary artery bypass using a cardiopulmonary bypass. Two other patients underwent an off-pump coronary artery bypass. Another two patients had valve procedures, and two underwent aortic repair using a cardiopulmonary bypass. The last patient was exposed to aortic repair as well as the CABG procedure. Therefore, 18 out of 20 patients were operated with the use of the cardiopulmonary bypass heart-lung machine and two were operated under beating heart conditions. Two out of the 20 patients were exposed to deep hypothermia. Three typical responses to the cardiovascular operation procedure are presented in Fig. 12.

In the first patient [shown in Fig. 12(a)], the responses of TBF and NADH were recorded as soon as the preparation for operation started with the scrubbing of the chest area (marked as A). This very early response was found only in one patient monitored in the cardiovascular operating room. The low level of TBF and the high level of NADH were recorded during the entire operation procedure, and the recovery began as soon as the chest was closed. When the patient left the operating room for the cardiac ICU, the two parameters were close to the baseline levels. These fast responses are probably due to high sensitivity and a fast response of the autonomic nervous system. We could speculate that the level of adrenaline was elevated very early, and as a result, the microcirculatory blood flow was decreased dramatically and the mitochondrial NADH became highly reduced. In the second patient who underwent the routine CABG operation [Fig. 12(b)], the same type of response was recorded. TBF reduction and NADH elevation were observed during most of the surgical procedure. Spontaneous transient recovery of TBF and NADH were noted during the second half of the operative procedure. In the third patient, operated on for aortic repair [Fig. 12(c)], clear responses to the procedure were recorded. In this patient, at 16:49, the initiation of extracorporeal circulation

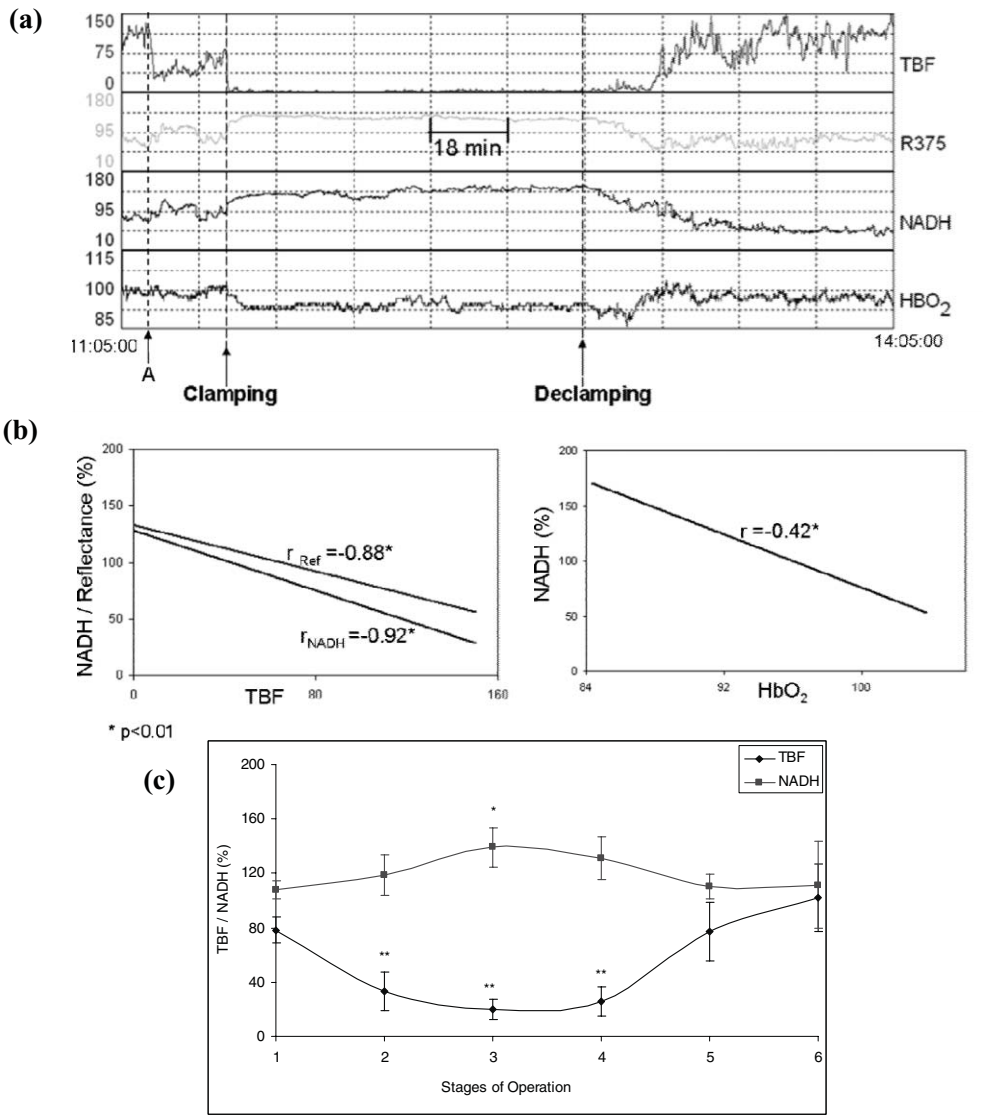

Fig. 11 (a) Effects of aortic occlusion in a patient that underwent an AAA repair operation, on the four parameters monitored by the CritiView. The technical preparation for aortic occlusion was performed at the marker A. (b) the correlations between TBF and NADH/reflectance or HbO_2 and NADH. (c) The Mean $\pm$ SE changes of TBF and NADH in five patients who underwent the AAA operation.

led to a large decrease in TBF and a large increase in NADH. The signals reverted toward the initial values, although the baseline was not reached (the monitoring period ended at 18:14). In order to perform statistical analysis, we selected patients that underwent a similar operation procedure. Only 13 patients were exposed to the same surgical protocol, and data were extracted from 11 patients. In two patients from the CABG normothermic group, the data collection was interrupted in the middle of the operation and we were unable to calculate the results to match the other 11 patients analyzed. The other seven patients were exposed to a different protocol and were not included in the statistical analysis. The Mean $\pm$ S.E. changes of TBF and NADH were obtained in 11 patients [Fig. 13(b)] following heart bypass operation during seven stages of the operation: Stage 1, 5 min baseline (after insertion of the catheter); stage 2, 10 min after chest opening; stage 3, 10 min after HLM or CPB was on; Stage 4, midpoint of HLM; stage 5, 10 min before HLM was off; stage 6, 10 min after HLM was off; and stage 7, the last 5 min of monitoring. ANOVA multiple comparison tests were conducted on the first three stages of the operation. Significance was found between points 1 and 3 in the TBF and between point 1 and points 2 and 3 in NADH ($*p < 0.05$, $**p < 0.01$, $n = 11$).

In one patient, it was possible to compare the responses of the urethral wall to ischemia induced under normothermic and hypothermic conditions. The results presented in Fig. 13 were measured in a patient who underwent aortic repair surgery. In the process of opening the chest, a major bleeding occurred and the patient was immediately put on the heart-lung machine and severe hypothermia was induced. As can be seen in Fig. 13(a), while the patient was normothermic, large changes in TBF and NADH were noted during the major bleeding event. After cooling the patient and shifting him to the heart-lung machine, the signals recovered, although the TBF remained under the control values. While the patient was hypothermic (17°C), the microcirculatory blood flow was directed mainly to the brain area [Fig. 13(b)], whereas the TBF to the urethra was decreasing

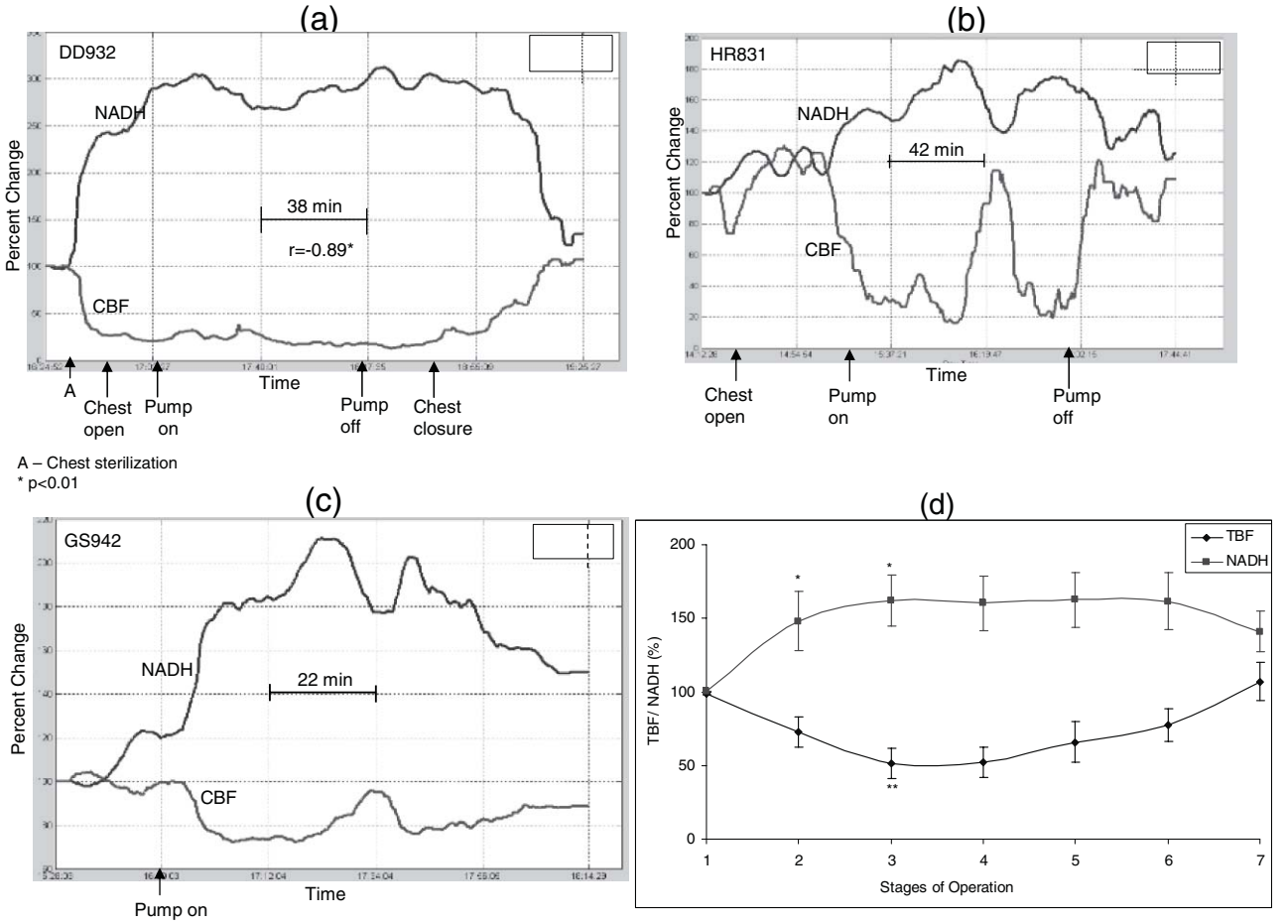

Fig. 12 Effects of the surgical procedure in (a–c) three cardiovascular operated patients on the urethral TBF and NADH redox state (see text for detailed explanations) and (d) the Mean ± SE changes of TBF and NADH in 11 patients during heart bypass operation.

significantly without any clear corresponding change in the NADH levels. This may suggest that the mitochondrial redox state behaves differently under hypothermia. It should be acknowledged that this response was recorded only in one patient.

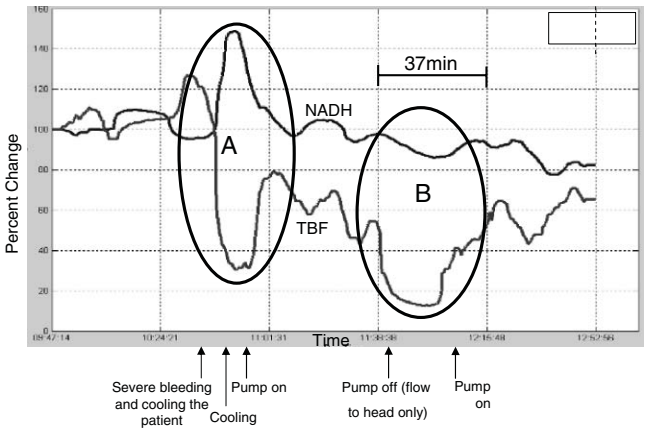

Fig. 13 Responses of the urethral wall TBF and NADH to systemic hypothermia (17°C) in a patient who underwent the aortic repair operation: (a) Responses to bleeding under normothermia and (b) responses to a decrease of microcirculatory blood flow to the lower part of the body.

4 Discussion

The main aim of this paper is to describe the development of the FDA-approved multiparametric monitoring system based on a laboratory device used in animal experiments. The present study demonstrates that the measures of local intracellular energy metabolism and microcirculatory blood flow assessed by an indwelling multiparameter sensor on a urethral catheter platform vary in a predictable fashion in response to transient severe changes in global and regional blood flow in patients exposed to cardiovascular surgery. Corresponding findings were obtained for the cerebral metabolism of gerbils. These semiquantitative data, presented as trends, suggest that changes in peripheral tissue perfusion may be detected rapidly and potentially before the occurrence of overt signs of end-organ hypoperfusion. Specifically, we were able to monitor the mitochondrial redox state, assessing the adequacy of oxygen balance in the urethral wall. We hypothesize that real-time monitoring of urethral mucosal NADH, measured concomitantly with urethral microcirculatory blood flow, may provide a rapid assessment of functional O_2 delivery. Insofar as elevated NADH is a sensitive measure of impaired visceral flow and tissue oxygen balance, the improvement of these parameters should indicate that other, metabolically more active organs have already replenished their oxygen debt.

The multiparametric monitoring of the tissue in real time has several advantages over single parameter measures. To evaluate the factors related to oxygen balance (supply/demand) in situations involving changes in O_2 supply to the tissue (i.e., ischemia or reperfusion), it is necessary to simultaneously assess a mitochondrial energy state, tissue O_2 saturation, and microcirculatory blood flow. The monitoring of tissue microcirculatory blood flow, in addition to mitochondrial NADH, using the LDF has been previously shown to be useful for both experimental and clinical settings.[84,85] Because the monitoring of the blood oxygenation level does not always reflect oxygen supply to the tissue, the present study monitored HbO_2 in the same location as the other parameters, namely, TBF and NADH. Nevertheless, the local monitoring of HbO_2 levels is not sufficient for an accurate evaluation of the balance between oxygen supply and demand, which is the key to tissue metabolism. In addition to TBF and HbO_2, we also monitored the most important parameter in energy metabolism, namely, the level of mitochondrial NADH.

It is important to emphasis that *in vivo* monitoring of mitochondrial function could be done measuring NADH, Fp, or cytochrome aa3. To date, in blood perused tissues only the NADH could be monitored relatively accurate by using the subtraction technique. It was never convincing that Fp and $Cytaa_3$ provide reliable data in blood perfused organs. The overlapping of the absorption spectra of hemoglobin and the Fp and the $Cytaa_3$ and the effects of blood volume or blood oxygenation could not be corrected properly. This issue was discussed in our review paper.[39]

Because the mitochondria play a main role in energy metabolism at the cellular level, monitoring changes in the mitochondrial NADH redox state reflects the state of tissue viability.[86] Thus, the simultaneous monitoring of the four parameters provides a clearer picture of the tissue viability and of the primary causes of energy failure if it is present, as has been previously validated by our group.[5,77,87]

In the present study, we chose the urethral mucosal tissue as a sampling site for two reasons: convenience and physiological rationale. This is a commonly instrumented site, and it would therefore involve no further invasion for continuous, long-term monitoring. The urethral tissue has a low metabolic rate and is not a preferential tissue for blood flow redistribution; thus, its metabolic activity should accurately reflect the final vascular bed flow restoration, without irreversible components, during resuscitation. This contrasts to intestinal mucosa, which can easily demonstrate irreversible injury, making it a poor indicator of global resuscitation effectiveness.

The concept that a single parameter could provide information on the adequacy of resuscitation is rapidly losing validity among clinicians. It is clear that, despite the numerous publications on gastric tonometry, this technique has achieved neither a wide acceptance nor clinical applicability. Perhaps even more important is the fact that, presently, there is no state-of-the-art method to assess when an optimal level of cellular homeostasis has been achieved and, hence, to ascertain that there is no further metabolic stress or ongoing energetic failure at the cellular level after various clinical perturbations.

Ideally, a monitoring strategy capable of providing real-time information on cell viability should fulfill a number of requirements. First, it should be based on highly reliable specific markers. Second, the system must allow for an easy and minimally or, preferably, noninvasive placement of the sensing element. It should be of low cost, low risk, and should provide a fast feedback in order to improve the treatment of the patient. Our study documents that the urethral mucosa, an easily accessible region, can be used to assess effective tissue perfusion in a less vital organ.

A primary limitation to this technique is its focus on a single monitoring site, the urethral mucosa. Because of variation in the vascular gradients, as well as O_2 gradients across the tissues, the monitored parameters may not represent adequately the real behavior of the tissue. Only by increasing the number of monitored sites in the tissue to three, we were able to collect better results during circulatory insufficiency states.

The data accumulated in the present preliminary study indicate that the CritiView device provides very clear results in performance tests under *in vitro* conditions as well as in small animal models. Testing the device in patients exposed to various cardiovascular surgical procedures produced fairly good preliminary results. We were aiming to correlate the real-time hemodynamic and respiratory parameters collected by the anesthesiology to the results collected by the CritiView. We found that this aim could be fulfilled after investing time and money to build a special data-logging system. In the meantime, we manually tested the possible correlation but were unable to conclude statistically significant data. We are planning to do this in our next clinical study. Nevertheless, in one patient presented in Fig. 10(c), we definitely found that our device provided an early warning signal to the deterioration of the patient due to the tamponade developed 3 h after the bypass operation. As seen in the right side of Fig. 10(c), the dramatic elevation in urethral wall NADH level was recorded, while the systemic blood pressure and heart beat were not significantly different.

The fact that the responses in the AAA patients to the occlusion procedure were inconsistent could be due to the following reasons:

(1) The urethra receives arterial flow directly from branches of the internal iliac and retrograde flow from branches that derivate from anastomoses between the superior and inferior mesenteric arteries. The origin of the superior mesenteric artery is situated in the abdominal aorta above the site of the clamping. (The inferior mesenteric artery is distal to the clamping.) In not all human subjects are these retrograde branches functional. This variation in the anatomy of blood vessels may explain why, in a few subjects, the decrease in microcirculatory blood flow occurred immediately after the occlusion (the retrograde branches are missing) and returned to the normal point after declamping. In other subjects, the retrograde flow may improve the level of TBF and saturation and decrease NADH during the occlusion period. In these subjects, the declamping led to the more rapid recovery of all four parameters to the normal level.

(2) Changes in blood volume due to bleeding (total blood loss that may be 500 ml up to 2–3 l) is a very important parameter with regard to changes in saturation, TBF, and NADH in subjects with a retrograde flow.

(3) Also, a decrease in temperature may induce supplemental vasoconstriction (that can be also produced by a rapid

and massive bleeding), which can change the real record of saturation.

Although the number of patients monitored during open chest surgery was very small, some initial suppositions could be made. The main premise in selecting this group was the assumption that this severe operation would induce changes in the oxygen balance in the body. If this is the case, then the viability assay of the urethral wall could be utilized during the operation and, more importantly, during the postoperative period (up to 24 h). As shown in Fig. 10(c), the monitoring of this patient postoperatively enabled us to detect early changes in body oxygen balance. Indeed, this patient developed a "tamponade" and NADH was elevated before the systemic parameters were clearly changed. This patient was moved to the operating room, and the reopening of the chest and solving the problem of accumulated blood inside the pericardium saved his life.

Another interesting case is the one presented in Fig. 12(c). As shown, the patient was moved to the cardiac intensive care unit (CICU) while the urethral wall did not recover to the baseline levels of NADH and tissue microcirculatory blood flow. Our monitoring ended at the end of the operation; thus, it was impossible to evaluate the viability of the urethral wall during the postoperative period. It was reported to us that this patient died after three days in the CICU.

These two cases provide preliminary indications suggesting that the monitoring of the urethral wall may have practical value in daily critical care medicine. It should be acknowledged, however, that the two patients constitute a very small number and, therefore, a large-scale clinical study is needed. We assume that most patients that will be monitored via the Foley catheter for the assessment of urethral wall viability will show a complete recovery at the end of the operation. Nevertheless, severely ill patients may deteriorate during the postoperative period and the deterioration should be detected as early as possible.

5 Conclusions

The new approach to monitor patients in critical care patients by CritiView was tested successfully under *in vitro* and animal *in vivo* experiments as well as in patients. The conclusions from this study are as follows:

(1) For the first time, NADH and microcirculatory blood flow and oxygenation was measured in the urethral wall of patients.

(2) Patients exposed to vascular and open chest surgeries showed changes in the measured parameters during the stressful condition of the body.

(3) The CritiView results may serve as early warning signals to the deterioration of the body or the end point of resuscitations during and after cardiovascular surgeries.

A large-scale clinical study with positive results may open up a new era in monitoring of critical care patients.

Acknowledgments

This paper is dedicated to the late Britton Chance who passed away November 16, 2010, at the age of 97. My collaboration (AM) with Chance started almost 40 years ago at the Johnson Research Foundation, University of Pennsylvania, Philadelphia. This study was supported by CritiSense Ltd. that had developed the CritiView.

References

1. M. D. Stern, "*In vivo* evaluation of microcirculation by coherent light scattering," *Nature* **254**, 56–58 (1975).
2. R. Bonner and R. Nossal, "Model for laser Doppler measurements of blood flow in tissue," *Appl. Opt.* **20**, 2097–2107 (1981).
3. A. P. Shepherd, "History of laser-Doppler blood flowmeter," in *Laser-Doppler Blood Flowmeter*, A. P. Shepherd and P. A. Oberg, Eds., pp. 1–16, Kluwer Academic, Dordrecht (1990).
4. J. E. Batista, J. R. Wagner, K. M. Azadzoi, R. J. Krane, and M. B. Siroky, "Direct measurement of blood flow in the human bladder," *J. Urol.* **155**, 630–633 (1996).
5. I. J. Rampil, L. Litt, and A. Mayevsky, "Correlated, simultaneous, multiple-wavelength optical monitoring *in vivo* of localized cerebrocortical NADH and brain microvessel hemoglobin oxygen saturation," *J. Clin. Monit.* **8**, 216–225 (1992).
6. A. Mayevsky, S. Lebourdais, and B. Chance, "The interrelation between brain PO_2 and NADH oxidation- reduction state in the gerbil," *J. Neurosci. Res.* **5**, 173–182 (1980).
7. D. W. Lubbers, "Optical sensors for clinical monitoring," *Acta Anaesth. Scand. Suppl.* **39**, 37–54 (1995).
8. I. E. Scheffler, "A century of mitochondrial research: achievements and perspectives," *Mitochondrion* **1**, 3–31 (2000).
9. A. Mayevsky, A. Deutsch, N. Dekel, E. Pevzner, and A. Jaronkin, "A new biomedical device for *in vivo* multiparametric evaluation of tissue vitality in critical care medicine," *Proc. SPIE* **5692**, 60–70 (2005).
10. A. Mayevsky, T. Manor, E. Pevzner, A. Deutsch, R. Etziony, N. Dekel, and A. Jaronkin, "Tissue spectroscope: a novel *in vivo* approach to real time monitoring of tissue vitality," *J. Biomed. Opt.* **9**, 1028–1045 (2004).
11. A. Mebazaa, A. A. Pitsis, A. Rudiger, W. Toller, D. Longrois, S. E. Ricksten, L. Bobek, S. De Hert, G. Wieselthaler, U. Schirmer, L. K. von Segesser, M. Sander, D. Poldermans, M. Ranucci, P. C. J. Karpati, P. Wouters, M. Seeberger, E. R. Schmid, W. Weder, and F. Follath, "Clinical review: practical recommendations on the management of perioperative heart failure in cardiac surgery," *Crit. Care* **14**, 201 (2010).
12. G. A. Ospina-Tascon, R. L. Cordioli, and J. L. Vincent, "What type of monitoring has been shown to improve outcomes in acutely ill patients?," *Intensive Care Med.* **34**, 800–820 (2008).
13. J. Creteur, T. Carollo, G. Soldati, G. Buchele, B. D. De, and J. L. Vincent, "The prognostic value of muscle StO_2 in septic patients," *Intensive Care Med.* **33**, 1549–1556 (2007).
14. J. A. Clavijo-Alvarez, C. A. Sims, M. R. Pinsky, and J. C. Puyana, "Monitoring skeletal muscle and subcutaneous tissue acid-base status and oxygenation during hemorrhagic shock and resuscitation," *Shock* **24**, 270–275 (2005).
15. M. R. Pinsky and D. Payen, "Probing the limits of regional tissue oxygenation measures," *Crit Care.* **13** (Suppl 5), S1 (2009).
16. D. C. Angus, W. T. Linde-Zwirble, J. Lidicker, G. Clermont, J. Carcillo, and M. R. Pinsky, "Epidemiology of severe sepsis in the United States: analysis of incidence, outcome, and associated costs of care," *Crit. Care Med.* **29**, 1303–1310 (2001).
17. C. Ince and M. Sinaasappel, "Microcirculatory oxygenation and shunting in sepsis and shock," *Crit. Care Med.* **27**, 1369–1377 (1999).
18. W. F. Ganong, *Review of Medical Physiology*, Appelton & Lange, Norwalk, CN (1991).
19. A. Barber, "Shock," in *Principles of Surgery*, S. I. Schwartz, Ed., pp. 101–122, McGraw-Hill, New York (1994).
20. R. Schlichtig, D. J. Kramer, and M. R. Pinsky, "Flow redistribution during progressive hemorrhage is a determinant of critical O_2 delivery," *J. Appl. Physiol.* **70**, 169–178 (1991).
21. A. Kraut, E. Barbiro-Michaely, and A. Mayevsky, "Differential effects of norepinephrine on brain and other less vital organs detected by a multisite multiparametric monitoring system," *Med. Sci. Monit.* **10**, BR215–BR220 (2004).
22. J. A. Clavijo, B. J. van, M. R. Pinsky, J. C. Puyana, and A. Mayevsky, "Minimally invasive real time monitoring of mitochondrial NADH and

tissue blood flow in the urethral wall during hemorrhage and resuscitation," *Med Sci Monit.* **14**, BR175–BR182 (2008).
23. A. T. Maciel, J. Creteur, and J. L. Vincent, "Tissue capnometry: does the answer lie under the tongue?," *Intensive Care Med.* **30**, 2157–2165 (2004).
24. P. E. Marik, "Sublingual capnometry: a non-invasive measure of microcirculatory dysfunction and tissue hypoxia," *Physiol. Meas.* **27**, R37–R47 (2006).
25. J. Creteur, "Gastric and sublingual capnometry," *Curr. Opin. Crit. Care.* **12**, 272–277 (2006).
26. S. P. Talpahewa, A. T. Lovell, G. D. Angelini, and R. Ascione, "Effect of cardiopulmonary bypass on cortical cerebral oxygenation during coronary artery bypass grafting," *Eur. J. Cardiothorac. Surg.* **26**, 676–681 (2004).
27. S. M. Millar, R. P. Alston, P. J. Andrews, and M. J. Souter, "Cerebral hypoperfusion in immediate postoperative period following coronary artery bypass grafting, heart valve, and abdominal aortic surgery," *Br. J. Anaesth.* **87**, 229–236 (2001).
28. J. Niinikoski and K. Kuttila, "Adequacy of tissue oxygenation in cardiac surgery: regional measurements," *Crit. Care Med.* **21**, S77–S83 (1993).
29. M. Haisjackl, J. Birnbaum, M. Redlin, M. Schmutzler, F. Waldenberger, H. Lochs, W. Konertz, and W. Kox, "Splanchnic oxygen transport and lactate metabolism during normothermic cardiopulmonary bypass in humans," *Anesth. Analg.* **86**, 22–27 (1998).
30. S. K. Ohri, J. Becket, J. Brannan, B. E. Keogh, and K. M. Taylor, "Effects of cardiopulmonary bypass on gut blood flow, oxygen utilization, and intramucosal pH," *Ann. Thorac. Surg.* **57**, 1193–1199 (1994).
31. S. K. Ohri, C. W. Bowles, R. T. Mathie, D. R. Lawrence, B. E. Keogh, and K. M. Taylor, "Effect of cardiopulmonary bypass perfusion protocols on gut tissue oxygenation and blood flow," *Ann. Thorac. Surg.* **64**, 163–170 (1997).
32. A. Perner, V. L. Jorgensen, T. D. Poulsen, D. Steinbruchel, B. Larsen, and L. W. Andersen, "Increased concentrations of L-lactate in the rectal lumen in patients undergoing cardiopulmonary bypass," *Br. J. Anaesth.* **95**, 764–768 (2005).
33. B. Chance, N. Oshino, T. Sugano, and A. Mayevsky, "Basic principles of tissue oxygen determination from mitochondrial signals," in *Oxygen Transport to Tissue*, pp. 239–244, Plenum Publ., New York (1973).
34. B. Chance and V. Legallias, "Rapid and sensitive spectrophotometry: a stopped-flow attachment for a stabilized quartz spectrophotometer," *Rev. Sci. Instrum.* **22**, 627–638 (1951).
35. B. Chance, "Spectra and reaction kinetics of respiratory pigments of homogenized and intact cells.," *Nature* **169**, 215–221 (1952).
36. B. Chance, "Spectrophotometry of intracellular respiratory pigments.," *Science* **120**, 767–775 (1954).
37. B. Chance and H. Baltscheffsky, "Respiratory enzymes in oxidative phosphorylation," *J. Biol. Chem.* **233**, 736–739 (1958).
38. B. Chance, P. Cohen, F. Jobsis, and B. Schoener, "Intracellular oxidation-reduction states *in vivo*," *Science* **137**, 499–508 (1962).
39. A. Mayevsky and G. G. Rogatsky, "Mitochondrial function *in vivo* evaluated by NADH fluorescence: from animal models to human studies," *Am. J. Physiol Cell Physiol.* **292**, C615–C640 (2007).
40. A. Mayevsky and B. Chance, "Oxidation-reduction states of NADH *in vivo*: From animals to clinical use," *Mitochondrion.* **7**, 330–339 (2007).
41. A. Mayevsky, "Brain NADH redox state monitored *in vivo* by fiber optic surface fluorometry," *Brain Res. Rev.* **7**, 49–68 (1984).
42. A. Mayevsky and B. Chance, "Intracellular oxidation-reduction state measured *in situ* by a multichannel fiber-optic surface fluorometer," *Science.* **217**, 537–540 (1982).
43. B. Chance, N. Oshino, T. Sugano, and A. Mayevsky, "Basic principles of tissue oxygen determination from mitochondrial signals," in *Oxygen Transport to Tissue. Instrumentation, Methods, and Physiology*, H. I. Bicher and D. F. Bruley, Eds., pp. 277–292, Plenum Publ., New York (1973).
44. D. W. Lubbers, "Optical sensors for clinical monitoring," *Acta Anaesth. Scand. Suppl.* **39**, 37–54 (1995).
45. A. Harden and W. Young, "The alcoholic ferment of yeast-juice," *Proc. R. Soc.* **77**, 405–120 (1906).
46. B. Chance and G. R. Williams, "A method for the localization of sites for oxidative phosphorylation," *Nature* **176**, 250–254 (1955).
47. B. Chance and G. R. Williams, "Respiratory enzymes in oxidative phosphorylation. III. the steady state," *J. Biol. Chem.* **217**, 409–427 (1955).
48. B. Chance, V. Legallias, and B. Schoener, "Metabolically linked changes in fluorescence emission spectra of cortex of rat brain, kidney and adrenal gland," *Nature* **195**, 1073–1075 (1962).
49. B. Chance and V. Legallias, "A spectrofluorometer for recording of intracellular oxidation- reduction states," *IEEE Trans. Biomed. Eng.* **BME-10**, 40–47 (1963).
50. F. F. Jobsis, M. O'Connor, A. Vitale, and H. Vreman, "Intracellular redox changes in functioning cerebral cortex. I. metabolic effects of epileptiform activity," *Neurophysiology* **34**, 735–749 (1971).
51. F. F. Jobsis and W. N. Stainsby, "Oxidation of NADH during contractions of circulated mammalian skeletal muscle," *Respir. Physiol.* **4**, 292–300 (1968).
52. E. Dora, L. Gyulai and A. G. B. Kovach, "Determinants of brain activation-induced cortical NAD/NADH responses *in vivo*," *Brain Res.* **299**, 61–72 (1984).
53. K. Harbig, B. Chance, A. G. B. Kovach, and M. Reivich, "*In vivo* measurement of pyridine nucleotide fluorescence from cat brain cortex," *J. Appl. Physiol.* **41**, 480–488 (1976).
54. C. Ince, J. M. C. C. Coremans, and H. A. Bruining, "*In vivo* NADH fluorescence," in *Oxygen Transport to Tissue XIV*, W. Erdmann and D. F. Bruley, Eds., pp. 277–296, Plenum Press, New York (1992).
55. R. S. Bradley and M. S. Thorniley, "A review of attenuation correction techniques for tissue fluorescence.," *J. R. Soc. Interface* **3**, 1–13 (2006).
56. K. H. Frank, M. Kessler, K. Appelbaum, and W. Dummler, "The Erlangen micro-lightguide spectrophotometer EMPHO I," *Phys. Med. Biol.* **34**, 1883–1900 (1989).
57. M. D. Stern, D. L. Lappe, P. D. Bowen, J. E. Chimosky, G. A. Holloway, Jr., H. R. Keiser, and R. L. Bowman, "Continuous measurement of tissue blood flow by laser-Doppler spectroscopy," *Am. J. Physiol.* **232**, H441–H448 (1977).
58. U. Dirnagl, B. Kaplan, M. Jacewicz, and W. Pulsinelli, "Continuous measurement of cerebral cortical blood flow by laser-Doppler flowmetry in a rat stroke model," *J. Cereb. Blood Flow Metab.* **9**, 589–596 (1989).
59. R. L. Haberl, M. L. Heizer, and E. F. Ellis, "Laser-Doppler assessment of brain microcirculation: effect of local alterations," *Am. J. Physiol.* **256**, H1255–H1260 (1989).
60. B. Chance and G. R. Williams, "Respiratory enzymes in oxidative phosphorylation. I. Kinetics of oxygen utilization," *J. Biol. Chem.* **217**, 383–393 (1955).
61. F. F. Jobsis, "Noninvasive, infrared monitoring of cerebral and myocardial oxygen sufficiency and circulatory parameters," *Science* **198**, 1264–1267 (1977).
62. M. S. Thorniley, S. Simpkin, E. Balogun, K. Khaw, C. Shurey, K. Burton, and C. J. Green, "Measurements of tissue viability in transplantation," *Philos. Trans. R. Soc. London B* **352**, 685–696 (1997).
63. A. J. Johnston and A. K. Gupta, "Advanced monitoring in the neurology intensive care unit: microdialysis," *Curr. Opin. Crit. Care* **8**, 121–127 (2002).
64. P. J. Hutchinson, "Microdialysis in traumatic brain injury—methodology and pathophysiology," *Acta Neurochir. Suppl.* **95**, 441–445 (2005).
65. P. J. Hutchinson, M. T. O'Connell, P. G. Al-Rawi, L. B. Maskell, R. Kett-White, A. K. Gupta, H. K. Richards, D. B. Hutchinson, P. J. Kirkpatrick, and J. D. Pickard, "Clinical cerebral microdialysis: a methodological study," *J. Neurosurg.* **93**, 37–43 (2000).
66. A. Zauner, E. Doppenberg, J. J. Woodward, C. Allen, S. Jebraili, H. F. Young, and R. Bullock, "Multiparametric continuous monitoring of brain metabolism and substrate delivery in neurosurgical patients," *Neurol. Res.* **19**, 265–273 (1997).
67. E. M. Doppenberg, A. Zauner, R. Bullock, J. D. Ward, P. P. Fatouros, and H. F. Young, "Correlations between brain tissue oxygen tension, carbon dioxide tension, pH, and cerebral blood flow–a better way of monitoring the severely injured brain?," *Surg. Neurol.* **49**, 650–654 (1998).
68. A. I. Maas, W. Fleckenstein, D. A. de Jong, and S. H. van, "Monitoring cerebral oxygenation: experimental studies and preliminary clinical results of continuous monitoring of cerebrospinal fluid and

brain tissue oxygen tension," *Acta Neurochir. Suppl. (Wien)* **59**, 50–57 (1993).
69. P. Lacombe, R. Sercombe, J. L. Correze, V. Springhetti, and J. Seylaz, "Spreading depression induces prolonged reduction of cortical blood flow reactivity in the rat," *Exp. Neurol.* **117**, 278–286 (1992).
70. R. K. van, H. Vermarien, and R. Bourgain, "Construction, calibration and evaluation of pO2 electrodes for chronical implantation in the rabbit brain cortex," *Adv. Exp. Med. Biol.* **316**, 85–101 (1992).
71. R. A. Van Hulst, D. Hasan, and B. Lachmann, "Intracranial pressure, brain PCO_2, PO_2, and pH during hypo- and hyperventilation at constant mean airway pressure in pigs," *Intensive Care Med.* **28**, 68–73 (2002).
72. B. Chance and B. Schoener, "Correlation of oxidation-reduction changes of intracellular reduced pyridine nucleotide and changes in electro-encephalogram of the rat in anoxia," *Nature* **195**, 956–958 (1962).
73. A. Mayevsky, Y. Blum, N. Dekel, A. Deutsch, R. Halfon, S. Kremer, E. Pewzner, E. Sherman, and O. Barnea, "The CritiView—a new fiber optic based optical device for the assessment of tissue vitality," *Proc. SPIE* **6083**, 60830Z (2006).
74. O. J. Kirkeby, I. R. Rise, L. Nordsletten, S. Skjeldal, C. Hall, and C. Risoe, "Cerebral blood flow measured with intracerebral laser-Dopplerflow probes and radioactive microspheres," *J. Appl. Physiol.* **79**, 1479–1486 (1995).
75. E. Dora, "Further studies on reflectometric monitoring of cerebrocortical microcirculation. Importance of lactate anions in coupling between cerebral blood flow and metabolism," *Acta Physiol. Hung.* **66**, 199–211 (1985).
76. A. Mayevsky, "The effect of trimethadione on brain energy metabolism and EEG activity of the conscious rat exposed to HPO," *J. Neurosci. Res.* **1**, 131–142 (1975).
77. A. Mayevsky, K. Frank, M. Muck, S. Nioka, M. Kessler, and B. Chance, "Multiparametric evaluation of brain functions in the Mongolian gerbil *in vivo*," *J. Basic Clin. Physiol. Pharmacol.* **3**, 323–342 (1992).
78. A. Mayevsky, D. Jamieson, and B. Chance, "Oxygen poisoning in the unanesthetized brain: correlation of the oxidation-reduction state of pyridine nucleotide with electrical activity," *Brain Res.* **76**, 481–491 (1974).
79. A. Mayevsky, "Shedding light on the awake brain," in *Frontiers in Bienergetics: From Electrons to Tissues*, P. L. Dutton, J. Leigh, and A. Scarpa, Eds., pp. 1467–1476, Academic Press, New York (1978).
80. A. Mayevsky, T. Manor, E. Pewzner, A. Deutsch, R. Etziony, and N. Dekel, "Real time optical monitoring of tissue vitality *in vivo*," *Proc. SPIE* **4616**, 30–39 (2002).
81. A. Mayevsky, T. Manor, E. Pewzner, A. Deutsch, R. Etziony, N. Dekel, and A. Jaronkin, "Tissue spectroscope: a novel *in vivo* approach to real time monitoring of tissue vitality," *J. Biomed. Opt.* **9**, 1028–1045 (2004).
82. A. Mayevsky, S. Meilin, T. Manor, E. Ornstein, N. Zarchin, and J. Sonn, "Multiparametric monitoring of brain oxygen balance under experimental and clinical conditions," *Neurol. Res.* **20**(Suppl 1), S76–S80 (1998).
83. A. Deutsch, E. Pewzner, A. Jaronkin, and A. Mayevsky, "Real time evaluation of tissue vitality by monitoring of microcircultory blood flow, HbO_2 and mitochondrial NADH redox state," *Proc. SPIE* **5317**, 116–127 (2004).
84. R. J. Andrews and R. P. Muto, "Retraction brain ischaemia: cerebral blood flow, evoked potentials, hypotension and hyperventilation in a new animal model," *Neurol. Res.* **14**, 12–18 (1992).
85. J. Hoper and M. R. Gaab, "Effect of arterial PCO_2 on local HbO_2 and relative Hb concentration in the human brain—a study with the Erlangen micro-lightguide spectrophotometer (EMPHO)," *Physiol. Meas.* **15**, 107–113 (1994).
86. J. M. Coremans, M. Van Aken, D. C. Naus, M. L. Van Velthuysen, H. A. Bruining, and G. J. Puppels, "Pretransplantation assessment of renal viability with NADH fluorimetry," *Kidney Int.* **57**, 671–683 (2000).
87. K. C. Wadhwani and S. I. Rapoport, "Blood flow in the central and peripheral nervous systems," in *Laser Doppler Blood Flowmetry*, A. P. Shepherd and P. A. Oberg, Eds., pp. 265–304, Kluwer Academic Pub., Boston (1990).